

This is a repository copy of Development of practical downsampling methods for nonlinear time history analysis of complex structures.

White Rose Research Online URL for this paper: https://eprints.whiterose.ac.uk/id/eprint/232754/

Version: Published Version

Article:

Majidi, N., Riahi, H.T. orcid.org/0000-0001-8891-1455, Zandi, S.M. et al. (1 more author) (2023) Development of practical downsampling methods for nonlinear time history analysis of complex structures. Soil Dynamics and Earthquake Engineering, 175. 108247. ISSN: 0267-7261

https://doi.org/10.1016/j.soildyn.2023.108247

Reuse

This article is distributed under the terms of the Creative Commons Attribution (CC BY) licence. This licence allows you to distribute, remix, tweak, and build upon the work, even commercially, as long as you credit the authors for the original work. More information and the full terms of the licence here: https://creativecommons.org/licenses/

Takedown

If you consider content in White Rose Research Online to be in breach of UK law, please notify us by emailing eprints@whiterose.ac.uk including the URL of the record and the reason for the withdrawal request.



ELSEVIER

Contents lists available at ScienceDirect

Soil Dynamics and Earthquake Engineering

journal homepage: www.elsevier.com/locate/soildyn





Development of practical downsampling methods for nonlinear time history analysis of complex structures

Noorollah Majidi^a, Hossein Tajmir Riahi^a, Sayed Mahdi Zandi^a, Iman Hajirasouliha^{b,*}

- a Department of Civil Engineering, University of Isfahan, Iran
- ^b Department of Civil and Structural Engineering, The University of Sheffield, UK

ARTICLE INFO

Keywords:
Downsampling methods
Discrete wavelet transform
Nonlinear time history analysis
Response spectrum
Hysteresis curve

ABSTRACT

One of the main problems of nonlinear time history analysis is its high computational effort, especially in structures with large number of structural components, high-rise buildings and complex structural systems. The ground motions recorded in recent years also include more recorded points than in the past, which has also increased the required volume of calculations. In this paper, three downsampling methods for reducing calculation costs of nonlinear time history analysis are presented and their applicability is investigated through practical examples of complex structures. These methods include the discrete wavelet transform, the time step correction, and the wavelet time step correction which is introduced in this paper. The efficiency of these downsampling methods is investigated for near-fault and far-fault earthquake records, as well as for records on different soil types. A comprehensive study is performed on five sets of ground motions consisting of 20 records. Each record is filtered up to three stages using one half, one quarter, and one eighth of the number of the main record points. First the linear and nonlinear response spectra based on the original records and the approximate waves are investigated. Subsequently, to evaluate the performance of the methods on more complex structural systems, two three-dimensional structures of 6-story and 15-story are analyzed. The 6-story structure is equipped with viscous dampers, while the 15-story structure has seismic isolators. The results indicate that the wavelet time step correction method has better performance in most cases, compared to the other two methods. It is shown that careful consideration is needed when dealing with earthquake records with high frequency contents. In such situations, one filtering step for the discrete wavelet transform method and two filtering steps for the other two methods are recommended. Also, in practical applications, it is advisable to choose earthquake records exhibiting the least error based on the results of SDOF systems analyses. Employing this technique can significantly cut down computational effort (up to 90%), while maintaining an average error ranging from 1% to 2% for the wavelet time step correction method.

1. Introduction

Time history analysis is the most accurate method to simulate the structural response to an earthquake record. However, this analysis is very time-consuming for structures with many structural components, high-rise buildings, and complex structural systems. On the other hand, the cost of calculations in nonlinear time history analysis is much higher than linear time history analysis. These obstacles limit the application of nonlinear time history analysis for practical design purposes. One of the key factors responsible for the high volume of calculations in time history analysis is the high number of recorded points for earthquake records. In Addition, in recent years, ground motions are recorded at

smaller time steps (in some cases smaller than 0.005 s), which increases the computational costs of calculations in this method. However, the necessity to use earthquake ground motion records with very small time steps is questionable for structures with high effective periods. For instance, in the case of high-rise structures that are generally more sensitive to long periods because of their fundamental period, the critical time step for numerical integration is longer than the recorded time step for the record [1,2]. Therefore, in such a structure, by increasing the time step of the earthquake record, the volume of calculations in time history analysis can be significantly reduced. However, the increment in the time step should be controlled to ensure the accuracy of the results will not be affected.

E-mail address: i.hajirasouliha@sheffield.ac.uk (I. Hajirasouliha).

^{*} Corresponding author.

Different methods have been proposed for reducing computational costs of dynamic analysis. These methods can be categorized into three general groups: (i) methods introducing new numerical methods for solving dynamic equations, (ii) methods using model simplification, and (iii) methods modifying the input ground motion record. Some of the examples of these three different approaches are given below.

Using the first approach, Lülf et al. [3] proposed a numerical method based on Ritz-vectors for nonlinear dynamic analysis of structures, which could significantly reduce the computational cost. Meyer and Matthies [4] also reduced computational costs of nonlinear dynamic analysis using Karhunen–Loeve and dual-weighted-residual methods. In another study, Toffolo et al. [5] proposed a method to reduce computational cost in dynamic fluid analysis. They reduced the volume of calculations in the thermoacoustic phenomenon by introducing a novel numerical method and modifying time steps. Adopting the second approach, Hemez and Doebling [6] reduced computational costs by simplifying a multi-degree of freedom system to a simpler system.

The third approach consists of truncation and downsampling methods. Truncation methods can reduce the length of an earthquake record in time history analysis based on its strong ground motion duration [7-10]. Generally, the strong ground motion duration of earthquake records is smaller than their total duration, and hence in truncation methods the weaker parts of the record (the first and the last parts) are omitted. However, the use of truncation methods can cause errors in nonlinear time history analysis, especially for structures near collapse limit state because these methods generally do not take into account the trailing weak ground motion, which may have significant effects on the nonlinear response of the structure. Downsampling methods use linear and nonlinear interpolations to increase the time step of an earthquake record. Soroushian [11] used a simple interpolation-based method to reduce the recorded ground motion points, which drastically improved the computational costs of the analysis of structures. In follow-up studies, Nateghi [12] used this method for dynamic analysis of a silo, while Soroushian et al. [13] used this method to reduce the calculation costs of analyzing a reservoir. Both studies showed the applicability of the method for real structures. Hosseini et al. [14] used the short-time Fourier transform to reduce computational efforts in analysis of SDOF structures. However, it should be noted that the above mentioned methods can increase the calculation error if they do not consider the frequency content of earthquake records in increasing time steps.

Wavelet transform is an efficient tool that can be used for analyzing data in the time and frequency domain [15]. This method has been adopted for generating approximate waves from a ground motion record in order to reduce the recorded points. For example, wavelet transform and Fourier transform were used by Salajegheh and Heidari [16] in order to reduce the computational costs of linear time history analysis of building structures. In another relevant study, the discrete wavelet transform was efficiency used to perform linear dynamic analysis, where acceptable results were obtained with lower computational costs [17]. They also used the wavelet neural network to reduce the cost of the optimization process of structures subjected to dynamic loads [18]. Heidari et al. [19] also utilized discrete wavelet transform in order to reduce calculation cost of linear dynamic analysis of shear-building structural systems. In another study, Heidari et al. [20]used the nonlinear response spectrum of single degree of freedom (SDOF) structures under a set of earthquake records by using a ductility factor. Their results, in general, demonstrated that the wavelet filter can be efficient in reducing the required computational costs. Similarly, Kaveh et al. [21] used wavelet transform for more efficient time history analyses and optimization of linear systems. Dadkhah et al. [22] also showed that the computational cost of incremental dynamic analysis (IDA) can be reduced by more than 87% using wavelet transform method.

Although in previous research studies, various methods have been presented to reduce the cost of time history analysis calculations, the limitations and error rates associated to these methods have not been compared for complex structural systems. In this paper, a comprehensive study is first conducted on the efficiency of two widely used methods in reducing the computational efforts of time history analysis calculations. Subsequently, a combined practical method with better performance is presented. To this end, the linear and nonlinear response spectra of single degree of freedom systems for 100 original earthquake records and modified ones are investigated. These ground motion records are selected from various geotechnical conditions to examine the accuracy of the studied methods. Finally, the response of two three-dimensional structures equipped with viscous dampers and seismic isolators under original records and modified ones are investigated to demonstrate the efficiency of each method in the case of complex real structures.

2. Research methodology

Using numerical integration methods to solve vibration problems in a time-domain analysis, suitable integration time step (Δt) for linear and nonlinear analyses can be obtained according to Equation 1-a [1] and Equation 1-b [2,23], respectively. In these equations, T is the period of the first mode of the structure, h is the largest integration time step for the stability of the numerical method [24] and $_f\Delta t$ is the time step of the earthquake acceleration record. In most time history analyses, the key parameter in the mentioned equations is $_f\Delta t$, which increases calculation costs. In recent years, the value of $_f\Delta t$ of the earthquake records has become smaller, which also increases the volume of calculations.

$$\Delta t \le Min\left(h, \frac{T}{10}, {}_f \Delta t\right) \tag{1-a}$$

$$\Delta t \leq Min\left(h, \frac{T}{100}, f\Delta t\right) \quad OR \quad \Delta t \leq Min\left(h, \frac{T}{1000}, f\Delta t\right)$$
 (1-b)

In this paper, three methods have been used to reduce the number of recorded points for each earthquake record. The first method is the discrete wavelet transform (DWT) which was first proposed by Salajegheh and Heidari [17]. The second method is called the time step correction (TSC) method, which was introduced by Soroushian [11] for downsampling. The third method, which is proposed in this paper, is a combination of the first and second method. In this section, the process of reducing earthquake recorded points in these three methods is presented.

2.1. Discrete wavelet transform (DWT or method 1)

Wavelet transform is a method to study the wave in the timefrequency domain. Using this method, in addition to the frequencies of a wave, the time of their occurrence can be also obtained. In earthquake engineering discipline, wavelet transform is generally used as a tool for time-frequency analysis of earthquake waves and production of artificial earthquake records. Lardies and Gouttebroze [25] used wavelet transform to represent the time-frequency response and determine the natural frequencies and mode shapes of structures. Similarly, Iyama and Kuwamura [26] utilized wavelet transform to analyze the time-frequency characteristics of earthquake records. Kiyani et al. [27] also performed time-frequency studies on earthquake records using continuous wavelet transform. Huang and Wang [28] used wavelet transform to generate artificial earthquake records compatible with a specific site. In another relevant study, Yamamoto and Baker [15] used wavelet packet transform to simulate the ground motion records, while Baker [29] adopted wavelet transform as a tool to classify near fault earthquakes. He et al. [30] used trigonometric wavelet transform as a shape function in numerical analysis of dynamic problems and compared it with an experimental sample. The proposed method showed compatible results with the experimental results. Jiang and Mahadevan [31] validated the frequency response of a structure in

numerical and experimental models using wavelet spectrum. The wavelet transform is also used by Schneider and Vasilyev [32]and Mahdavi and Abdul Razak [33] to solve problems related to fluid dynamics and dynamic analysis of space frames, respectively.

Wavelet transform can also be used in dynamic analysis of structures to reduce computational costs by increasing time step of earthquake records. Previous research shows that this method has good performance in linear and nonlinear dynamic analysis of structures [16–20,22, 34–38]. Using wavelet transform, an approximate wave of the main earthquake record with fewer recorded points is made and it is used for dynamic analysis of structures. Using two characteristics of scale and shift, the wavelet transform can extract time and frequency information of the wave at the same time. According to Fig. 1, it can be seen that using the wavelet transform, the time of occurrence of different frequencies can be extracted. Wavelet transform is divided into two general categories: discrete and continuous. Shift and scale parameters are discrete and continuous in discrete and continuous wavelet transform, respectively. However, for discrete waves in time, continuous wavelet transform can also be used.

Generally, the discrete wavelet transform is used to filter earthquake acceleration records, while continuous wavelet transform (CWT) is mostly used for time-frequency studies. CWT is defined according to equation (2) [40].

$$X_{WT}(\tau, s) = \frac{1}{\sqrt{s}} \int_{-\infty}^{+\infty} x(t) \psi^* \left(\frac{t - \tau}{s}\right) dt$$
 (2)

In Equation (2), the continuous wavelet function is obtained based on two parameters, shift (τ) and scale (s). In this equation, x(t) represents the input wave over time, while the mother function is represented

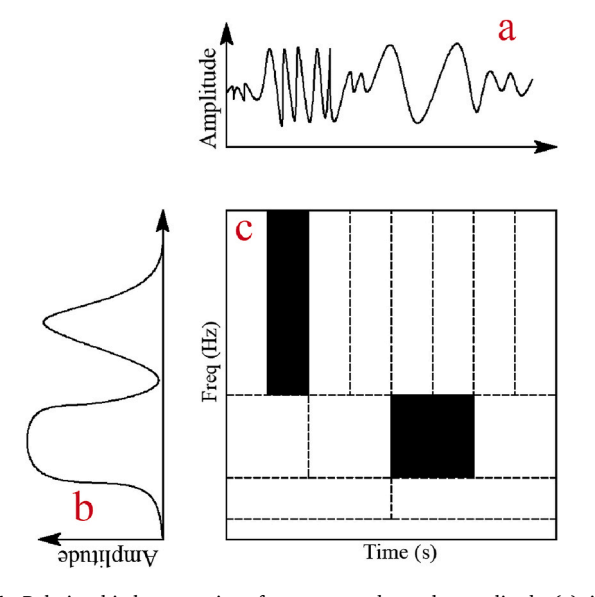


Fig. 1. Relationship between time, frequency, and wavelet amplitude: (a) time-series, (b) Fourier spectrum, and (c) wavelet transform.

by ψ^* (* indicates it is a complex function). Based on this equation, the scale and shift parameters change continuously.

Using discrete wavelet transform (DWT), waves can be converted into a series of low-pass and high-pass filters. The main purpose of this study is to reduce the recorded points of an earthquake record by converting it into two waves with high and low frequencies. Therefore, the DWT method was adopted by using the Haar wavelet function as the mother function, as suggested by previous studies for filtering earthquake records [17–19,22,36]. In Equation (3), the mother function $(\psi^*(t))$ and the scale function $(\varphi(t))$ used in this study are presented as follows:

$$\psi^*(t) = \begin{cases} 1 & 0 \le t < 0.5 \\ -1 & 0.5 \le t < 1 \\ 0 & otherwise \end{cases}$$
 (3-a)

$$\varphi(t) = \begin{cases} 1 & 0 \le t \le 1 \\ 0 & otherwise \end{cases}$$
 (3-b)

As shown in Fig. 2, for a signal (S), which in this paper is the earthquake acceleration record, the number of points is assumed to be equal to N. The signal is then converted into two high-pass (D1) and lowpass (A1) waves using the DWT. The high-pass wave represents the wave of details, while the low-pass wave indicates the wave of approximations. Due to the fact that the wave of details includes high frequencies of earthquake records, it can be ignored considering an appropriate degree of accuracy. By removing the wave of details in each step, the number of input signal points is reduced to half of the number of points in the previous step. Therefore, in each step, the wave of approximations can be divided to low-pass and high-pass, while in the next step, only the low-pass part will be utilized. Previous studies demonstrated the good performance of this approach in reducing the computational costs of dvnamic analysis [16-20,22,34-38]. In this study, earthquake acceleration records are filtered up to three steps using the DWT method (see Fig. 2). Therefore, the number of points for waves A1 to A3, which are used instead of the main earthquake record, is one half, one quarter, and one eighth of the main one, respectively.

The waves A and D can be calculated using the following equations, as recommended by Mallat [39]:

$$A_{j} = \sum_{n} S(n)g_{j}^{*}(n - 2^{j}k)$$

$$j = 1, 2, \dots \quad k = 1, 2, \dots$$
(4)

$$D_{j} = \sum_{n} S(n) h_{j}^{*} (n - 2^{j}k)$$

$$j = 1, 2, \dots \quad k = 1, 2, \dots$$
(5)

$$h_1(n) = h(n) \tag{6}$$

$$g_1(n) = g(n) \tag{7}$$

$$h_{j+1}(n) = \sum_{k} h_j(k)g(n-2k)$$
 (8)

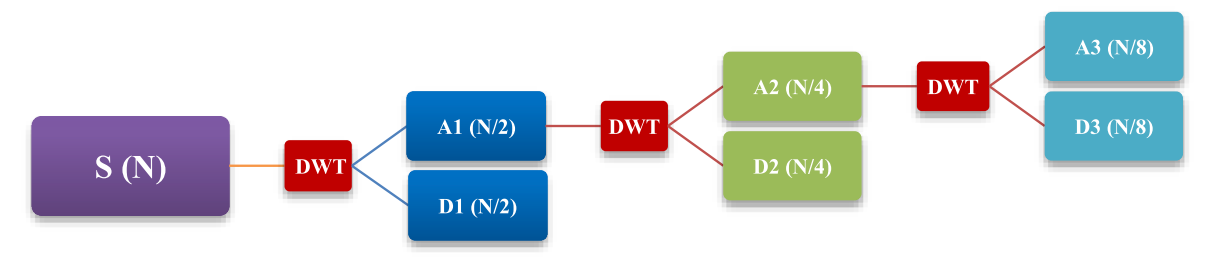


Fig. 2. Steps of the DWT method used in this study.

$$g_{j+1}(n) = \sum_{k} g_j(k)g(n-2k)$$
(9)

In the above equations, g_j and h_j denote high-pass and low-pass and filters, respectively [40]. Filters g_j and h_j are computed using Equations (6)–(9). The indices j, k, and n are integer counters. In each step, the S wave is calculated based on Equation (10). Parameter j in this equation represents the filter step

$$S = A_j + \sum_{i=1}^{j} D_i$$
 $j = 1, 2, 3, ...$ (10)

Using the above equations, the wave of approximations can be obtained based on the DWT method.

2.2. Time step correction (TSC or method 2)

Using downsampling methods, increasing the time step of earth-quake records is acceptable as long as the results converge to the exact solution with a good level of accuracy. In 2008, Soroushian [11] presented a downsampling method named time step correction (TSC) to approximate earthquake records. In follow-up studies [11,41–45] he demonstrated the performance of the TSC method for linear and nonlinear analyses of regular and irregular structures in plan and height. The performance of this method in near-field and far-field earthquake records was also investigated [46]. According to the results, this method has a good performance in different types of structures. The proposed method can reduce the cost of calculations up to 90% with an error of less than 7% [41].

As shown in Fig. 3, in the TSC method, the main earthquake record, $f(t_i)$, is converted to the approximate wave, \widetilde{f}_i . In this process, the time step of the main record $({}_f\Delta t)$ is converted to ${}_f\Delta\widetilde{t}=n_f\Delta t, n\in\{2,3,...\}$ (time step of the approximate wave). The approximate wave in this method is obtained based on Equation (11) [11]:

$$\widetilde{f}_{i} = \begin{cases}
g(t_{i}) & t_{i} = 0 \\
\frac{1}{2}g(t_{i}) + \frac{1}{4n'} \sum_{k=1}^{n'} \left[g(t_{i+k/n}) + g(t_{i-k/n}) \right] & 0 < t_{i} \le t'_{end} \\
g(t_{i}) & t_{i} = t'_{end}
\end{cases}$$
(11)

In Equation (11), n' is obtained from the following equation:

$$n' = \begin{cases} n - 1 \\ \frac{n}{2} & n = 2j, j \in Z^{+} \\ \frac{n-1}{2} & n = 2j + 1, j \in Z^{+} \end{cases}$$
 when $t_{i} = n_{f} \Delta t$ when $t_{i} \neq n_{f} \Delta t, t_{i} \neq t'_{end} - n_{f} \Delta t$ when $t_{i} = t'_{end} - n_{f} \Delta t$
$$n - 1$$
 (12)

 $t_{\rm end}^{\prime}$ should satisfy the two conditions given in Equations (13) and 14).

$$t_{end} \le t_{end}' < t_{end} + n_f \Delta t \tag{13}$$

$$\frac{\dot{t}_{end}}{n_f \Delta t} \in \{1, 2, \ldots\} \tag{14}$$

 $g(t_i)$ is then obtained from Equation (15):

$$g(t_{i}) = \begin{cases} f(t_{i}) & \text{when } 0 < t_{i} \le t_{end} \\ 0 & \text{when } t_{end} \le t_{i} \le t_{end} \end{cases}$$
 (15)

In the above equation, t_{end} is the duration of the original record. The

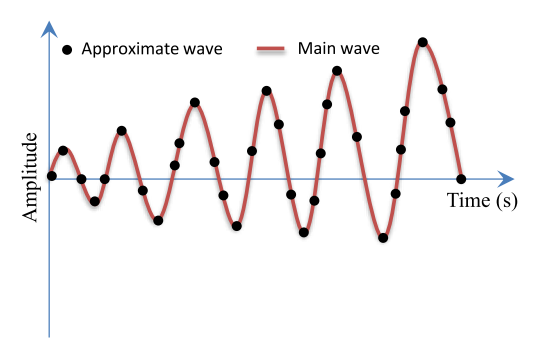


Fig. 3. Typical pattern of conversion of the main wave to the approximate wave in the TSC method.

parameter n in Equation (12) represents the magnification scale of the time step for the approximate wave. To ensure that the magnification scale does not affect the accuracy of the calculations, this number should be chosen in such a way that the time step of the approximate wave is not greater than the time step obtained from Equation (1) [24]. The largest value that can be considered for n (n_{max}) is given by Equation (16).

$$n_{\max_f} \Delta t \le Min\left(\Delta t_{cr}, {}_f \Delta t, \frac{T}{x}\right) < (n_{\max} + 1)_f \Delta t$$

$$n_{\max} \in \{2, 3, 4, \dots\}$$
(16)

In Equation (16), Δt_{cr} represents the largest time step for the stability of the numerical solution method, T is the effective period of the structure obtained from modal analysis, and x is equal to 10 for linear analysis and 100 and 1000 for nonlinear analysis neglecting or considering impact effects, respectively [41]. In this study, the value of n for the approximate wave A1 to A3 is assumed to be 2, 4, and 8, respectively (see Fig. 4). In this figure, S (N) is the main record with the total number of N data points, which is converted to A1 to A3 approximate waves using the TSC method. The number of data points of A1, A2 and A3 is one half, one quarter, and one eighth of S (N), respectively. This is similar to the DWT method and makes it possible to compare the results.

2.3. Wavelet time step correction (WTSC or method 3)

In this section, a new method is presented for improving the performance of the previous two methods. In the DWT method, in each wavelet filter stage, the wave of approximations of the previous stage is used. In each stage of the filter, by removing the wave of details, the number of wave points of the new approximation becomes half of the previous stage. Previous studies showed that removing the wave of details in the second and third stage creates error and the first stage wave of approximations has the best performance since it is extracted from the main record directly. In addition, in the TSC method, the frequency content is not directly considered in the process of making approximate waves, and hence the frequency content of the main record may be lost.

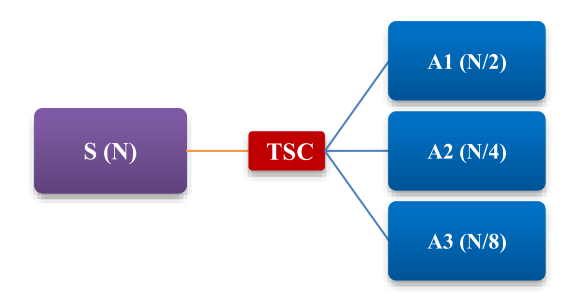


Fig. 4. Time step correction approximate waves.

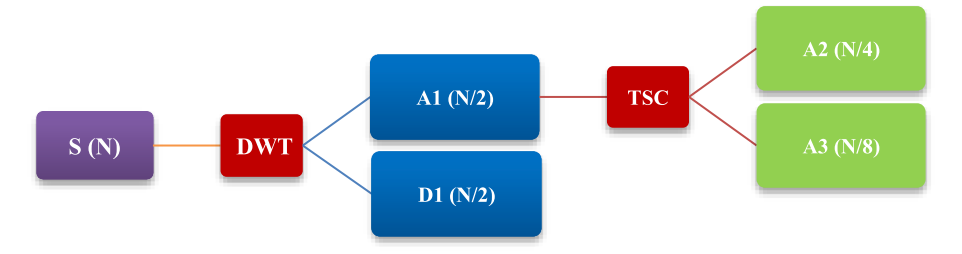


Fig. 5. The WTSC method approximate waves.

Therefore, it is expected that combining these two concepts together will reduce errors in the computational process. The combined method proposed in this study is called Wavelet Time Step Correction (WTSC) hereafter. In this method, an approximate wave (A1) of the main earthquake record is generated using the DWT method, and therefore, it is the same as A1 in the DWT method. The second and the third approximate waves (A2 and A3) are then generated from A1 using the TSC method (see Fig. 5). The number of data points of A1, A2 and A3 is similar to approximate waves of the DWT and the TSC methods.

3. Analysis of single degree of freedom (SDOF) systems

To evaluate the performance of the three mentioned methods in the previous section, first the linear and nonlinear acceleration spectra for the main records and their approximate waves are compared. For this purpose, different sets of earthquake records of FEMA 440 [47] are used. These record sets correspond to four different sites, representing class B. C, D and E (very soft) soil conditions. The fifth set corresponds to earthquake records influenced by near fault effects. Each set contains 20 earthquake records. In this paper, the acceleration spectra of different sets for behavior factors of 1, 2, 4, 6, and 8 are obtained. In the following, the results obtained from each method are presented separately. In the tables and figures presented, main represents the results obtained from the main earthquake records, while A1 to A3 represents the results obtained from approximate waves. In the following, for different methods, the maximum error for the average response spectrum of each set is calculated. This error is obtained based on equation (17). In equation (17), parameters $S_{Main,R}$ and $S_{Aj,R}$ are the average acceleration response spectrum of the main earthquake records and approximate waves for the behavior factors R, respectively.

$$E_{Aj,R}^{\text{max}}\left(\%\right) = \max\left(\left|\frac{S_{Main,R} - S_{Aj,R}}{S_{Main,R}}\right|\right) \times 100\tag{17}$$

3.1. Results of the DWT method

In this section, the acceleration response spectra of different earth-quake records are studied using the DWT method. As mentioned before, at each stage of the wavelet transform, the detail wave, which includes high frequencies of the main wave, is removed from the calculations. Thus, if the predominant frequency content of the earthquake record includes high frequencies, application of the DWT method may lead to considerable errors. Fig. 6 shows the acceleration wave for two main earthquake records and their wavelet filters (from the Loma Prieta and the Northridge earthquakes). As can be seen, in the Loma Prieta earthquake record, waves of details have small amplitudes up to the third stage. On the other hand, in the Northridge earthquake record, the wave of details in the first stage of the wavelet filter has a high amplitude.

Therefore, it can be expected that the wavelet filter has a better performance in the case of the Loma Prieta earthquake record. In Fig. 6, A1 to A5 and D1 to D5 waves show the waves of approximations and details of the first to the fifth stages of the wavelet filter, respectively. As can be seen, in the fourth and the fifth stages, the amplitude of the wave of details is approximately equal to the wave of approximations. Therefore, in this study the wavelet transform is only used up to the third stage. This conclusion is consistent with the findings of Heidari et al. [37] and Dadkhah et al. [22].

Fig. 7 compares the elastic acceleration response spectra of the Loma Prieta and the Northridge earthquakes for the main records and the approximate waves. Response spectra for all approximate waves of the Loma Prieta earthquake record are well matched with the main record spectrum, while for the Northridge earthquake record, A2 and A3 waves response spectra are not in good agreement with the main record response spectrum. According to Fig. 7, only A1 approximate wave can be used instead of the main record of the Northridge earthquake with acceptable error.

It can be seen from Figs. 6 and 7 that if the wave of details has a high amplitude, its effects cannot be disregarded and using the wave of approximation may lead to unacceptable errors. This indicates that if the frequency content of the main record includes high frequencies, its wave of details will have an important role in the characteristics of the record. To demonstrate this, the Fourier spectra of the mentioned earthquake records are plotted in Fig. 8. This figure shows that the Fourier spectrum for the Northridge earthquake record has a significant amplitude for frequencies up to 10 Hz, while the frequency content of the Loma Prieta earthquake is limited to frequencies below 5 Hz. Studies have shown that the DWT method has a better performance for earthquakes whose frequency content includes low-pass frequencies [22,36]. This principle can be used in selecting the number of wavelet filters for the main earthquake record and also to find out that the DWT method can be applied on which records. The large difference in the acceleration response spectrum of the A3 wave for the Northridge earthquake record makes the use of the DWT method ambiguous. However, it is necessary to study this issue for different earthquake records, which will be explained in the following.

Fig. 9 compares the mean elastic acceleration response spectra of different record sets for the main records and approximate records obtained using the DWT method. It can be seen that the results are, in general, in good agreement, and especially for A1 and A2 approximate waves, response spectra are well matched. In most record sets, the maximum difference between the main and approximate records response spectra occurred in periods less than 1 s, and for structures with longer periods the error was negligible. Using A2 wave instead of the main earthquake record in all sets, and using A3 wave instead of the main earthquake record in very soft soils and near-fault sets led to a

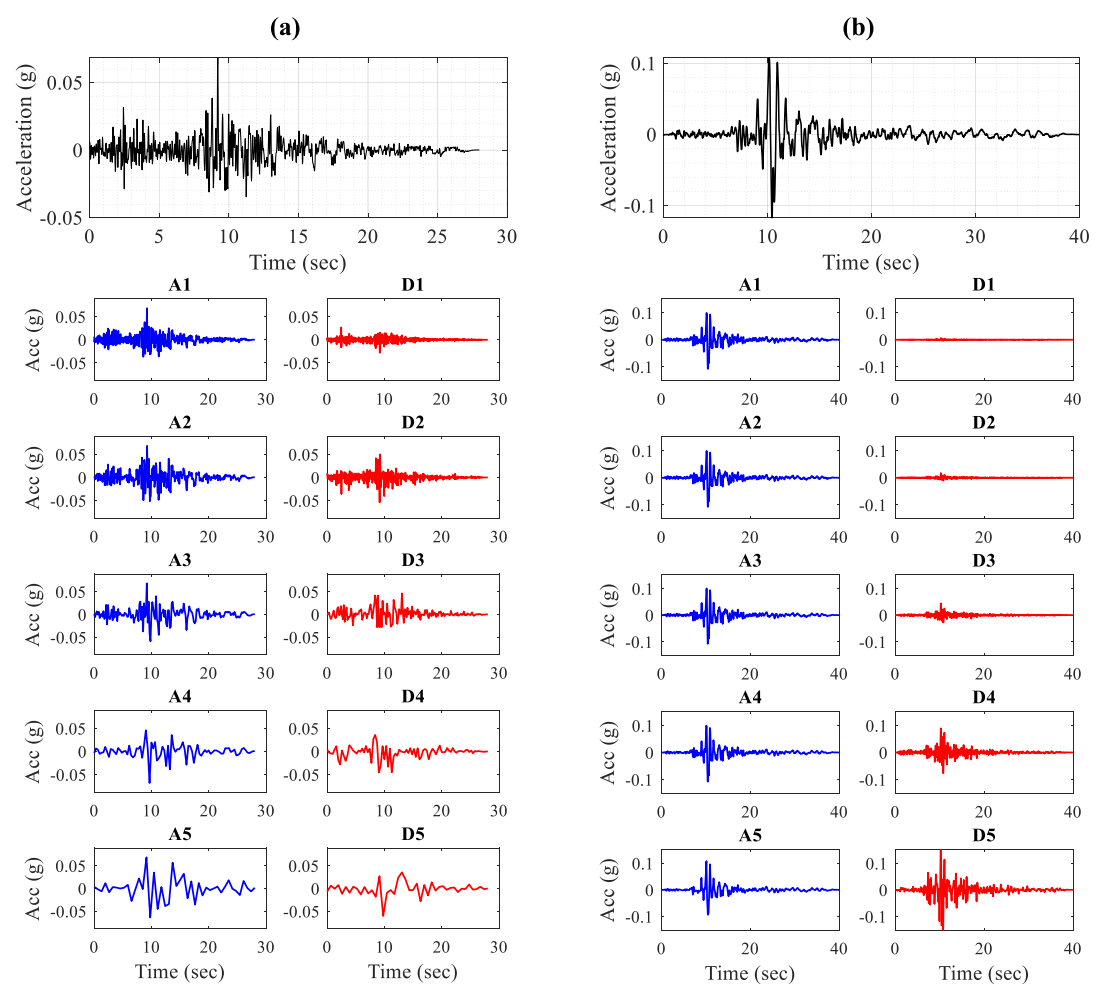


Fig. 6. Main acceleration records and wavelet filters of: (a) the Northridge earthquake (NRATB090) and (b) the Loma Prieta earthquake (LPBRK090) both recorded on soil type B.

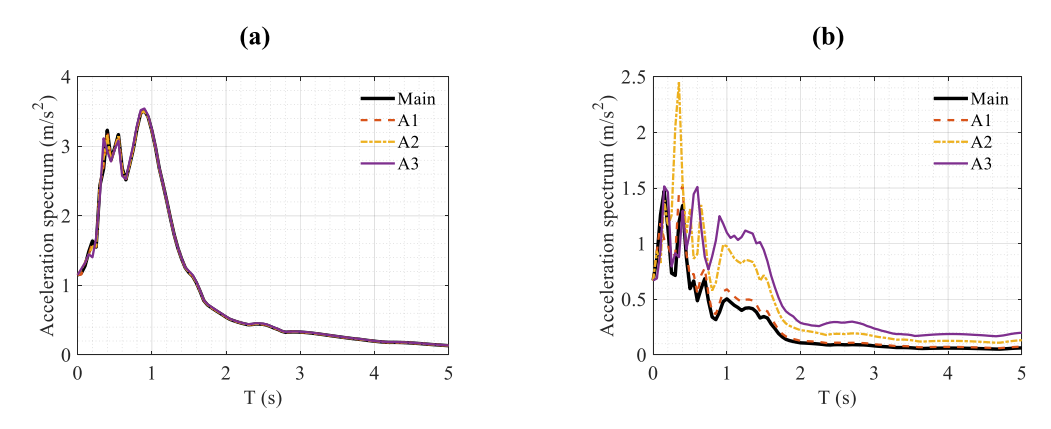


Fig. 7. Acceleration response spectra of main records and wavelet filters for (a) the Loma Prieta earthquake record (LPBRK090) and (b) the Northridge Earthquake record (NRATB090).

small error in calculating response spectrum.

Given the promising results of the A3 wave in estimating the elastic response spectrum, this wave is examined to predict the inelastic response spectrum in Fig. 10. In this figure, the mean elastic and inelastic response spectra (R $=1,\,2,\,4,\,6,\,8$) for A3 waves are compared with those of the main records. The results confirm the proper agreement of the response spectrum obtained from A3 waves and main

records and only in the record sets of soil type B and D, the difference between the results can be noticed. Again, the largest error in estimating the response spectrum is related to systems that have a period of less than 1 s. Also, by increasing the nonlinear behavior of the systems (i.e. increasing the behavior factor), the error of using the DWT method is generally reduced.

Table 1 presents the maximum error of estimating the mean

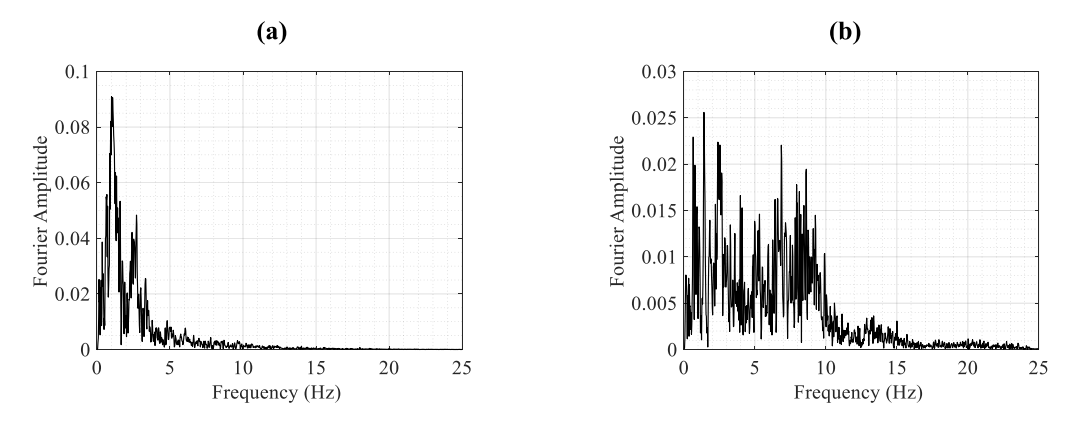


Fig. 8. Fourier spectrum for (a) the Loma Prieta earthquake record (LPBRK090) and (b) the Northridge earthquake record (NRATB090).

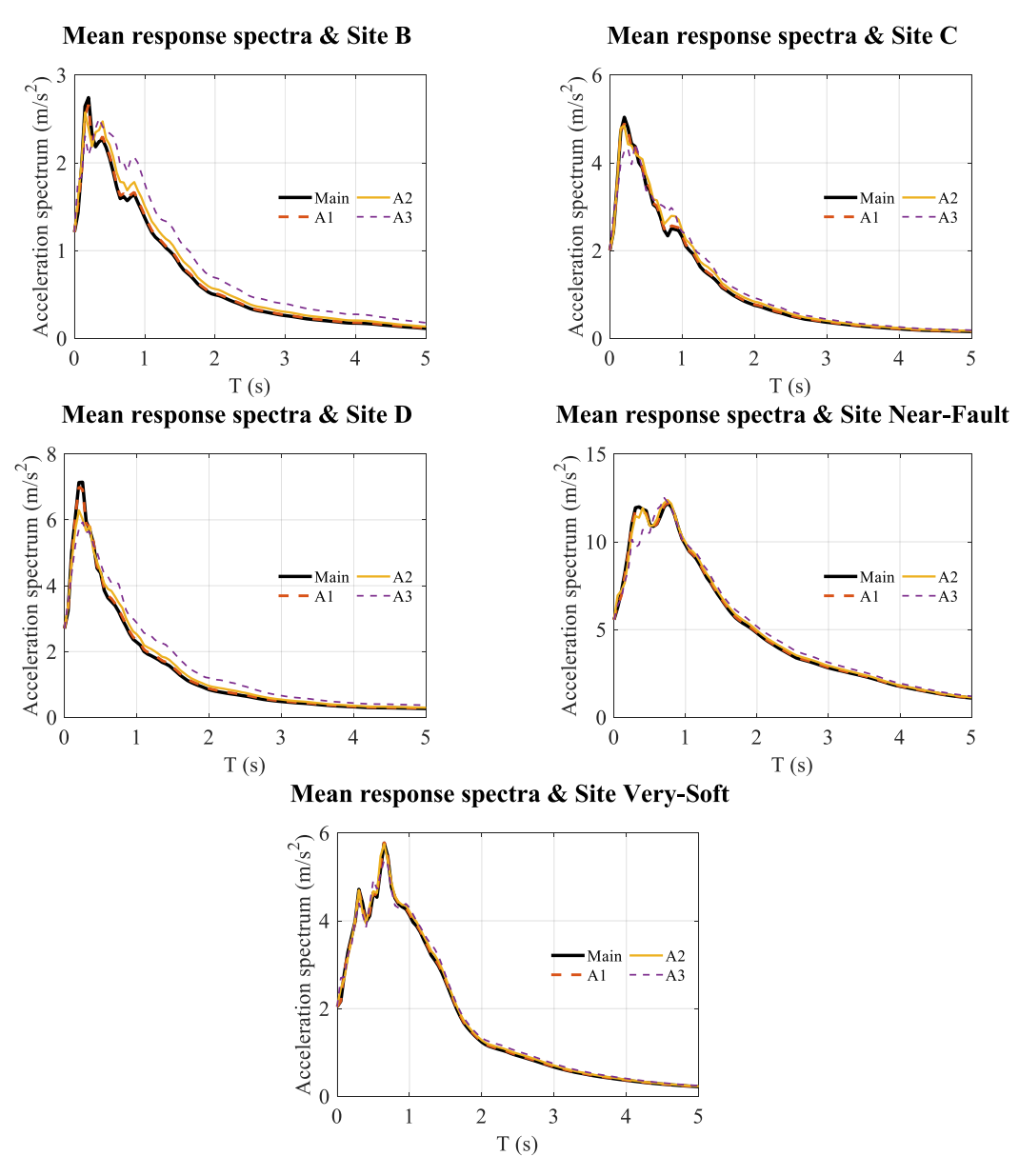
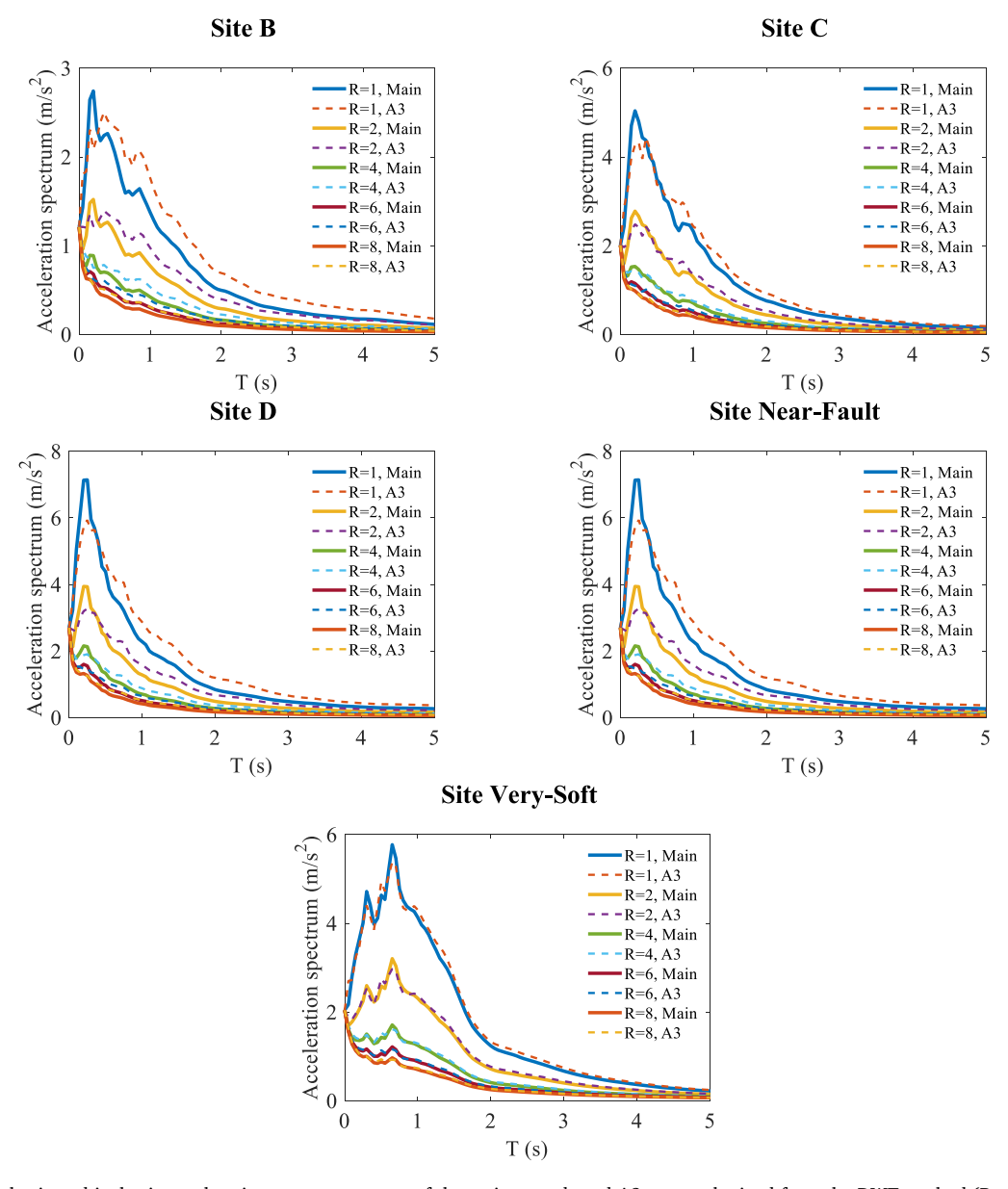


Fig. 9. Mean elastic acceleration response spectra of the main records and approximate ones obtained from the DWT method.



 $\textbf{Fig. 10.} \ \ \text{Mean elastic and inelastic acceleration response spectra of the main records and A3 waves obtained from the DWT method (R=1, 2, 4, 6, and 8). \\$

acceleration response spectra by using A1, A2, and A3 waves for different behavior factors in the period range of 0–5 s. Like the previous results, at all sites and for all approximate waves, the maximum error decreases with increasing behavior factor (increasing nonlinearity). The maximum errors of A1, A2, and A3 waves in all sets of records are 8%, 18%, and 58%, respectively, which mostly occurs in estimating the elastic response spectrum. According to the results presented in Table 1, the maximum error of the DWT method for A2 waves and especially A3 waves is high, which indicates the use of this wave for some records should be done with extreme caution.

3.2. Results of the TSC method

Fig. 11 shows the acceleration of the original record and the approximate records obtained from the TSC method for the Loma Prieta and Northridge earthquakes. Similar to the DWT method, the approximate waves of the Loma Prieta earthquake record are well-matched with the original record, however this is not the case for the Northridge earthquake record. For a better comparison of the two methods, the

acceleration response spectra of the approximate records by the TSC method and the main records are compared in Fig. 12 for the two mentioned earthquakes. Comparing this figure with Fig. 7 indicates that the performance of the TSC method is generally better than the DWT method for earthquake records with high frequency content. Besides, Fig. 12 shows that in the Northridge earthquake record, A2 wave leads to an acceptable error while in the DWT method only A1 wave is acceptable.

Fig. 13 compares the mean elastic acceleration response spectra of different record sets for the main records and approximate records obtained using the TSC method. The agreement between the resulting spectra is appropriate and again in this method, the maximum error occurs in systems with a period less than 1 s. The A3 waves obtained by the TSC method generally have better performance than the A3 waves obtained by the DWT method, and these waves have the best performance in very soft soil and the worst performance in soil type B records set. As a general conclusion, the use of A3 waves in this method is acceptable leading to reasonable errors. In the DWT method, the acceleration response spectra of the approximate records are higher than

 Table 1

 Maximum error of different sites for the DWT method.

Maximum error o	f mean acceleration spectrum	for soil type B (%)			
Wave	R = 8	R = 6	R = 4	R = 2	R = 1
A1	8.09	7.41	6.37	8.38	6.51
A2	13.90	14.51	15.36	16.43	18.10
A3	47.51	48.87	51.19	52.81	58.24
Maximum error o	f mean acceleration spectrum	for soil type C (%)			
Wave	R = 8	R = 6	R = 4	R = 2	R = 1
A1	2.58	2.71	3.18	3.45	3.11
A2	12.61	13.06	13.63	13.47	15.37
A3	19.21	19.63	19.97	22.85	23.08
Maximum error o	f mean acceleration spectrum	for soil type D (%)			
Wave	R = 8	R = 6	R = 4	R = 2	R = 1
A1	4.09	4.21	4.37	4.48	4.87
A2	13.58	14.30	14.73	15.31	16.24
A3	39.28	41.05	43.68	46.82	48.86
Maximum error o	f the mean acceleration spectr	um for the near-fault site (%)			
Wave	R = 8	R = 6	R = 4	R = 2	R = 1
A1	0.97	0.98	1.33	2.15	2.93
A2	3.32	3.65	3.92	6.46	11.03
A3	8.69	9.94	10.46	17.88	18.92
Maximum error o	f mean acceleration spectrum	for very soft soil (%)			
Wave	R = 8	R = 6	R = 4	R = 2	R = 1
A1	1.22	1.29	1.35	1.87	2.03
A2	4.74	4.99	4.99	5.76	13.52
A3	9.14	9.04	9.49	10.91	24.55

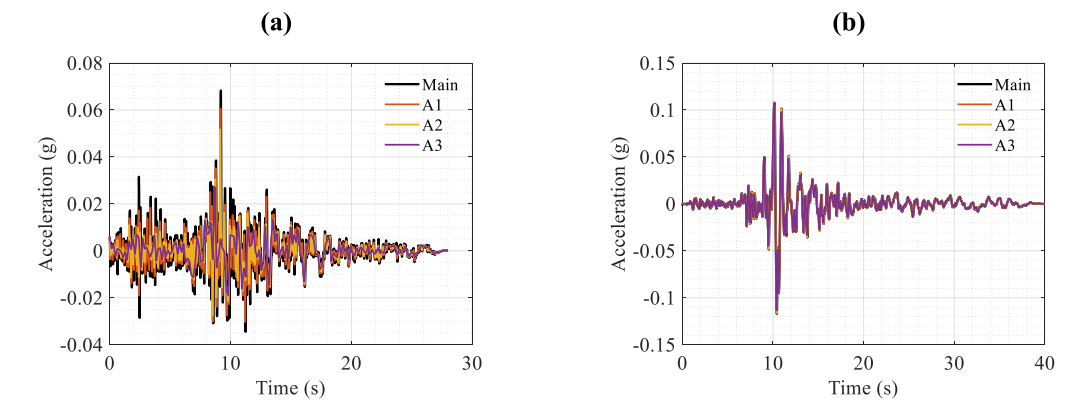


Fig. 11. Main acceleration records and the TSC method approximate waves of (a) the Northridge earthquake (NRATB090) and (b) the Loma Prieta earthquake (LPBRK090).

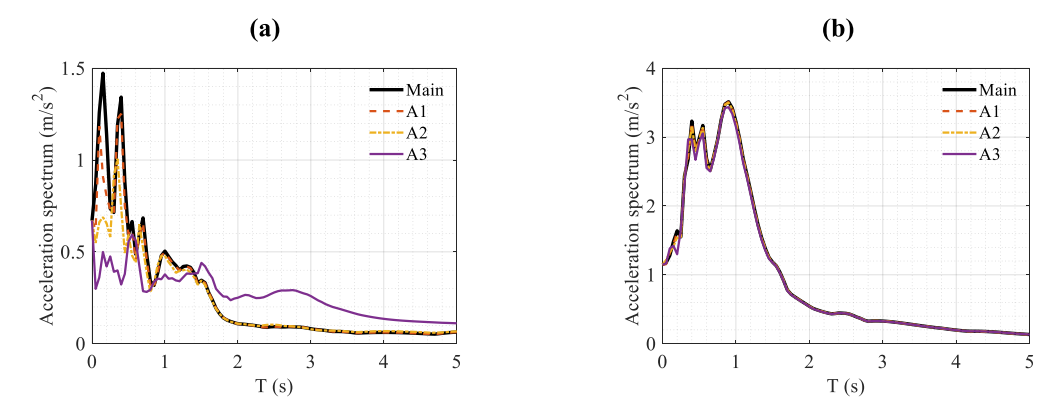


Fig. 12. Acceleration response spectra of main records and the TSC method approximate waves for (a) the Loma Prieta earthquake (LPBRK090) and (b) the Northridge earthquake (NRATB090).

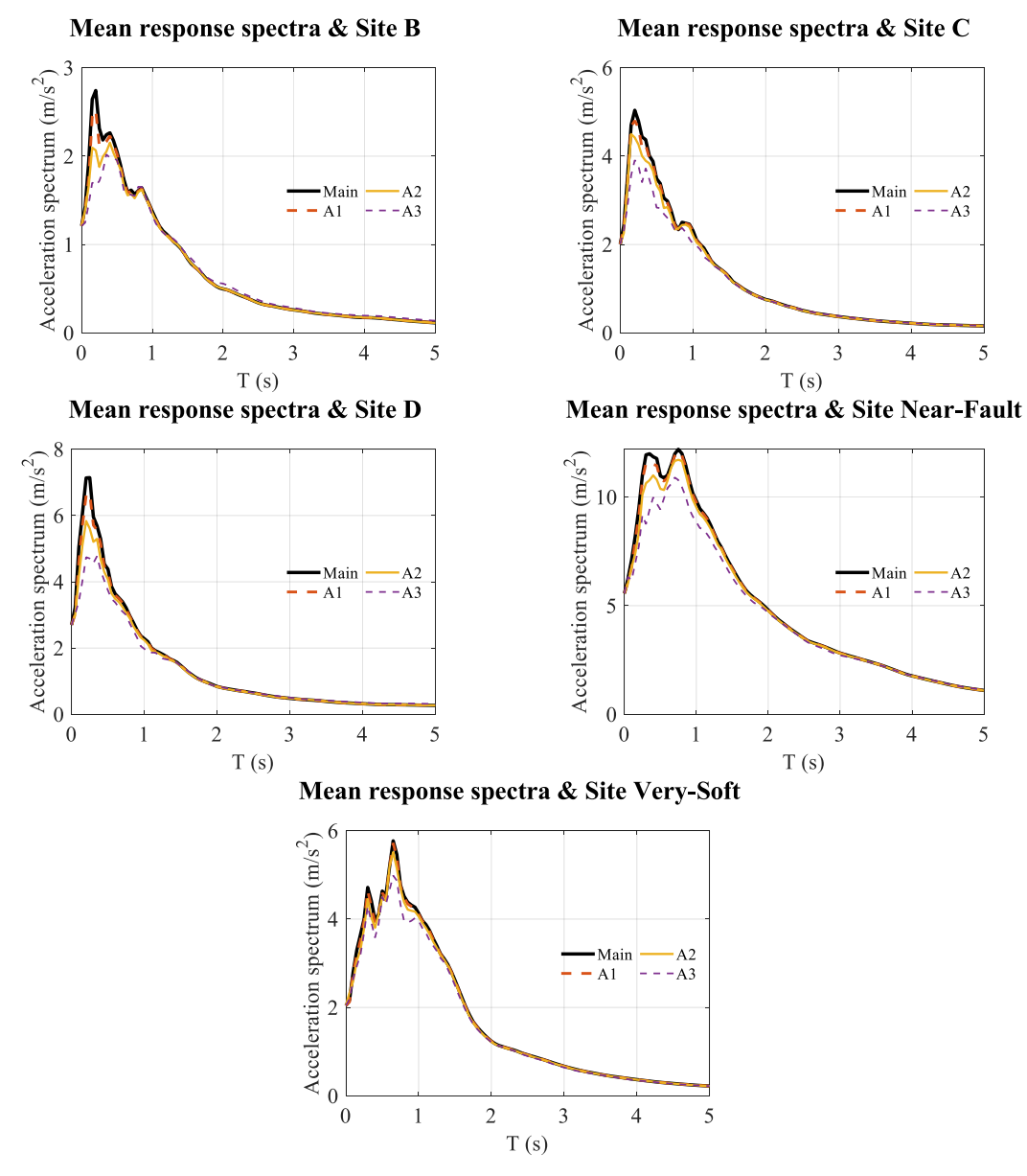


Fig. 13. Mean elastic acceleration response spectra of the main records and approximate ones obtained from the TSC method.

the response spectra of the main records, but this is opposite in the TSC method. As a result, application of the TSC method should be done with caution as it may lead to considerable errors.

Fig. 14 compares the mean of the elastic and inelastic acceleration response spectra for the A3 waves of the TSC method with the corresponding main records response spectra. The compatibility of the response spectra is appropriate for the A3 wave at all sites and for all behavior factors, which is especially evident for systems having a period more than 1 s. It can be also noted that by increasing the behavior factor of the systems, the error of using the TSC method is reduced.

Table 2 presents the maximum error of estimating the mean acceleration response spectra by A1, A2 and A3 waves obtained from the TSC method for different behavior factors in the period range of 0–5 s. The maximum errors of A1, A2, and A3 waves in all sets of records are 10, 25, and 39%, respectively, which mostly occurs in estimating the elastic response spectrum. Comparing the maximum error of the DWT method with the TSC method shows that the maximum error of the TSC method for the A3 wave is significantly lower in soil types B, C, and D. However, in very soft soil sites and near-fault earthquake events, in some cases, the

maximum error of the DWT method is less than the TSC method.

3.3. Results of the WTSC method

In this section, the adequacy of the approximate records obtained using the WTSC method are examined. It is worth noting that since A1 wave in this method is obtained using the DWT method, this wave is the same as A1 wave of the DWT method. Fig. 15 compares the mean elastic acceleration response spectra for different record sets of the main records and their corresponding approximate records obtained using the WTSC method. By comparing this figure with Figs. 13 and 9, it can be concluded that this method can also provide a good estimate of the response spectra of the main records. Similar to the TSC method, the approximate waves acceleration response spectra have values less than the main record response spectra. In this method, the A3 waves have the best performance in very soft soil (type E) and the worst estimate for soil type B. For structures with a period of more than 1 s, this method outperforms the DWT and TSC methods. Fig. 16 compares the mean elastic and inelastic acceleration response spectra for the A3 waves obtained

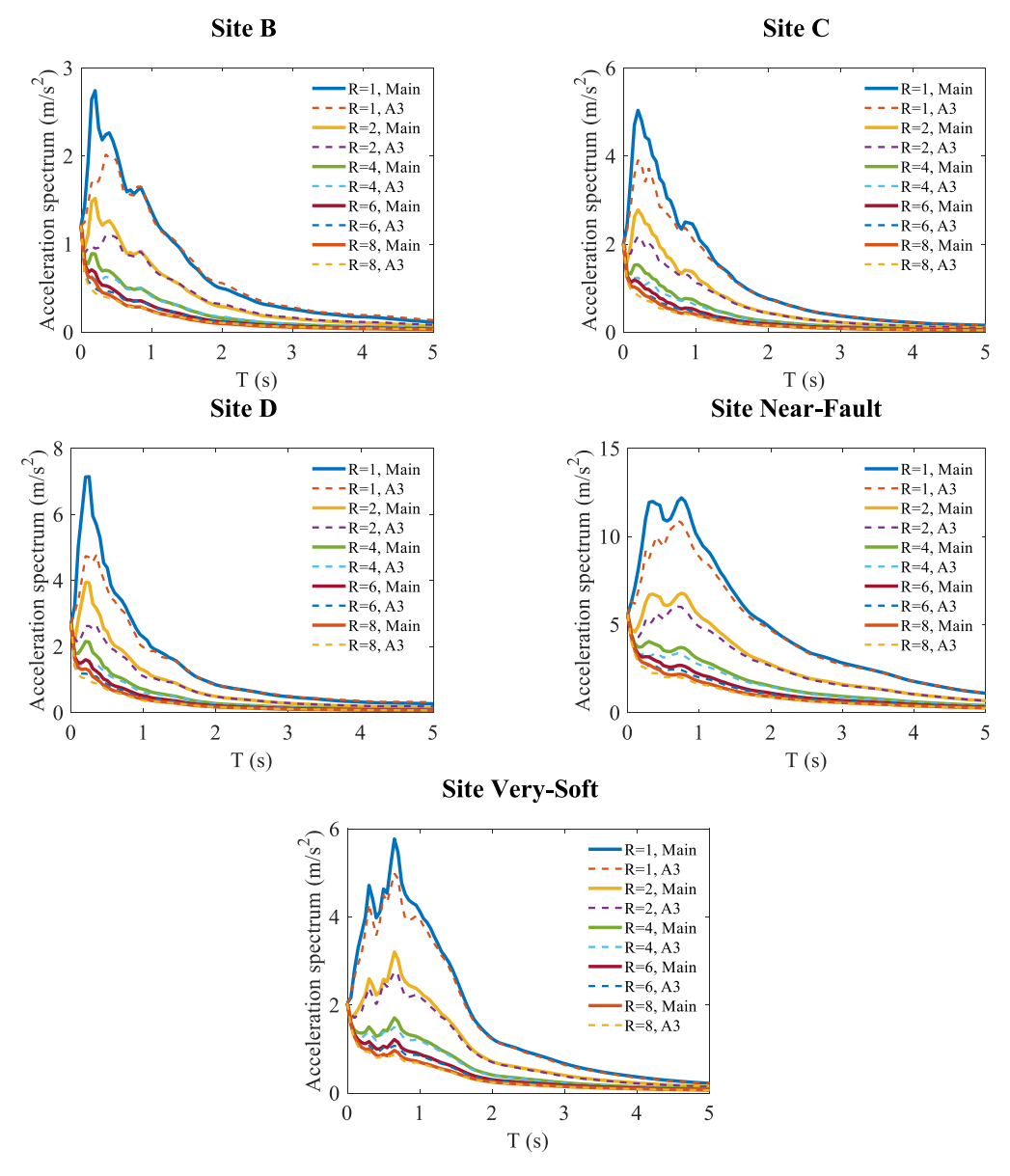


Fig. 14. Mean elastic and inelastic acceleration response spectra of the main records and A3 waves obtained from the TSC method (R = 1, 2, 4, 6, and 8).

from the WTSC method and the main records response spectra. Comparison between this figure with Figs. 10 and 14, confirms the results discussed before.

Table 3 presents the maximum error of estimating the mean acceleration response spectra by using A1, A2 and A3 waves obtained from the WTSC method. The maximum errors of A1, A2, and A3 waves in all sets of records are 8%, 25%, and 42%, respectively, which mostly occurred in estimating the elastic response spectra. Comparing the maximum error in the DWT method with the WTSC method shows that the maximum error of the WTSC method for the A3 wave is significantly lower. It can be noted that the maximum error of this method for the A3 wave in most cases is similar to the TSC method.

3.4. Investigation of the average error of A3 waves in different methods

This section aims to examine the accuracy of the proposed methods for a wide range of periods. Due to the fact that the A3 wave obtained by the TSC and the WTSC methods showed good performance, the average error of A3 waves in different methods is considered as the main crite-

rion calculated by using Equation (18). In this equation, E, n, and R are the number of earthquake records, the number of single degree of freedom (SDOF) systems with equally spaced periods ranging from 0 to 5 s, and the number of behavior factors, respectively. Moreover, $S_{ire,Main}$ represents the calculated acceleration response spectrum for the main ground motion records, while $S_{ire,A3}$ is the corresponding value form the A3 wave.

$$Er_{mean} = \left| \left(\left(\frac{1}{E} \times \frac{1}{n} \times \frac{1}{R} \right) \sum_{e=1}^{E} \sum_{r=1}^{R} \sum_{i=1}^{n} \frac{S_{ire,Main} - S_{ire,A3}}{S_{ire,Main}} \right) \times 100 \right|$$

$$E = 20, n = 101, R = 5$$
(18)

Fig. 17 shows the mean error of different methods for different behavior factors and different sites. The results indicate that the average error for the TSC method and the WTSC method is significantly lower than the DWT method. The average error for the two methods of TSC and WTSC in all sites is in the range of 5–10%. Unlike the maximum error, which decreased with increasing the behavior factors, the trend of changes in the average error in different sites is not the same. It can be

Table 2
Maximum error of different sites for the TSC method.

Maximum error o	f mean acceleration spectrum	for soil type B (%)				
Wave	R = 8	R = 6	R = 4	R = 2	R = 1	
A1	6.02	6.74	7.59	9.13	9.83	
A2	16.54	19.42	22.46	24.57	24.70	
A3	23.13	26.94	32.67	37.61	39.19	
Maximum error o	f mean acceleration spectrum	for soil type C (%)				
Wave	R = 8	R = 6	R = 4	R = 2	R = 1	
A1	3.00	3.08	4.59	5.18	5.59	
A2	8.40	8.73	10.48	12.47	12.27	
A3	14.48	17.71	20.32	22.75	24.18	
Maximum error o	f mean acceleration spectrum	for soil type D (%)				
Wave	R = 8	R = 6	R = 4	R = 2	R = 1	
A1	5.07	5.56	7.28	7.63	8.53	
A2	15.25	17.22	19.32	21.39	21.52	
A3	23.50	26.28	28.71	33.46	34.16	
Maximum error o	f the mean acceleration spectr	um for the near-fault site (%)				
Wave	R = 8	R = 6	R = 4	R = 2	R = 1	
A1	2.57	2.59	3.20	3.99	4.97	
A2	6.58	8.11	8.80	11.74	12.05	
A3	15.86	17.63	20.69	25.18	26.72	
Maximum error o	f mean acceleration spectrum	for very soft soil (%)				
Wave	R = 8	R = 6	R = 4	R = 2	R = 1	
A1	1.87	1.85	1.85	3.23	3.38	
A2	5.15	5.63	5.90	8.36	9.40	
A3	10.27	11.46	12.48	13.97	13.61	

judged that increasing the time step by 8 times in all linear and nonlinear analyses using both the TSC and the WTSC methods is very efficient. Also, the error of the WTSC method is often less than the other methods, which confirms its higher efficacy.

4. Computational cost for different approximate waves

As mentioned before, the number of approximate wave points of A1, A2 and A3 is one half, one quarter, and one eighth of the main earth-quake records, respectively. This reduction in the number of points is expected to reduce the cost of calculations. Table 4 shows the calculation time (in seconds) of the acceleration response spectrum for different behavior factors. As mentioned earlier, each site contains a set of 20 earthquake records. The time presented for each site in Table 4 is the total calculation time to obtain the acceleration response spectrum of 20 earthquake records. Since the computation times for different methods were relatively close, the following results are only presented for the WTSC method. It can be seen that using A3 wave in most cases reduced the cost of analysis by more than 80%.

5. Seismic performance of structures based on approximate waves

It was shown in previous sections that the application of presented downsampling methods can greatly improve the computational efficiency of time history analysis. But in some earthquake records, the resulting error was not acceptable, which highlights the importance of the selection of earthquake records that are suitable for downsampling. To enhance the precision of downsampling techniques in practical implementations, it is advisable to assess their impact on the outcomes of SDOF systems, and subsequently choose the most effective ones for practical application of more complex MDOF systems. In this section, the practical application of the proposed downsampling methods in complex structural systems is investigated by selecting the most suitable earthquake records. Seven earthquake records are selected from 40 records of soil type C and D sets, as a minimum recommended number by

most seismic codes for time history analysis of the structures [48]. The selected records are chosen to have the lowest mean error in all the three downsampling methods in SDOF systems, while the error of all methods is not necessarily equal. Table 5 presents the characteristics of the selected earthquake records. To assess the efficiency of the proposed downsampling methods for practical applications, two complex structures, one equipped with viscous dampers and the other one equipped with seismic isolators are considered. It is assumed that these structures are located on a site with $S_{\rm S}, F_{\rm a}, S_{\rm 1}$ and $F_{\rm v}$ equal to 1.4, 1.0, 0.5 and 1.8, respectively, based on ASCE 7 [48]. The selected records are scaled based to be consistent with the seismic hazard level of the site.

Previous studies showed that the time history of velocity is one of the important characteristics of ground motion records [1,49,50]. Therefore, Fig. 18 shows the time history of velocity of the main and approximate selected records using different downsampling methods. In general, it can be seen that in the DWT method, the time history of velocity is in very good agreement with the main earthquake record. However, in the TSC method, in some earthquake records (E(1) and E (4)), the time history of velocity of the A3 wave is slightly different from that of the main record. This difference (error) is reduced in the WTSC method

5.1. Structure equipped with viscous dampers

In this section, the results of a 6-story steel structure equipped with viscous dampers is presented. The plan of the structure is adopted from FEMA P-1051 [51] as shown in Fig. 19. The viscous dampers are designed based on the method presented by Christopoulos and Filiatrault [52]. Accordingly, in the first and second stories of each frame equipped with the dampers, two 50 kip $-\sec/inch$ viscous dampers are used while for the other stories, one 50 kip $-\sec/inch$ viscous damper is utilized. The values of λ_{max} and λ_{min} (representing possible total variation in damper properties above or below the nominal values) are considered to be 1.15 and 0.85, respectively [51]. The plan of the structure and the view of the frames equipped with the dampers are shown in Fig. 19.

Time history analyses were performed using the seven selected

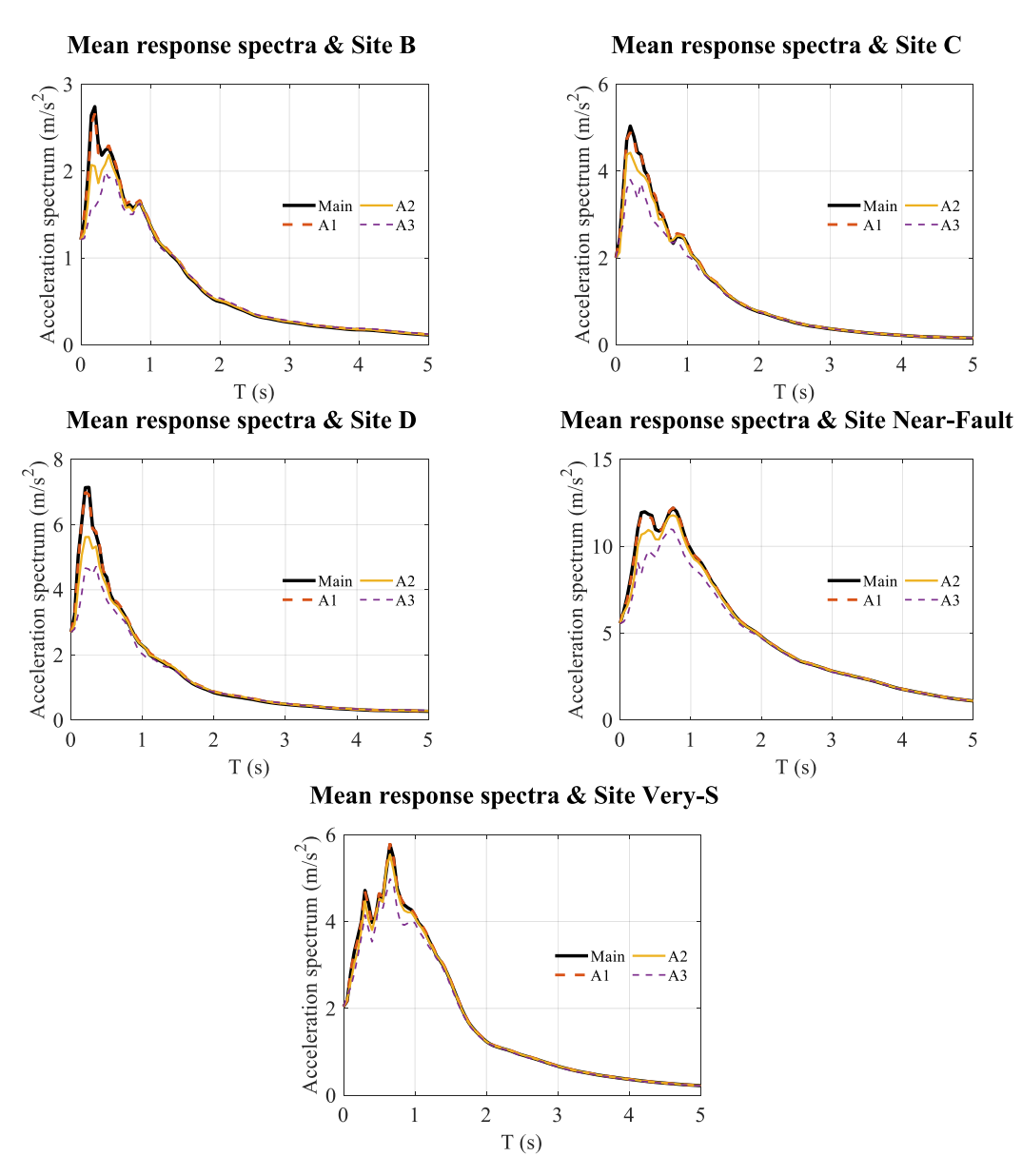
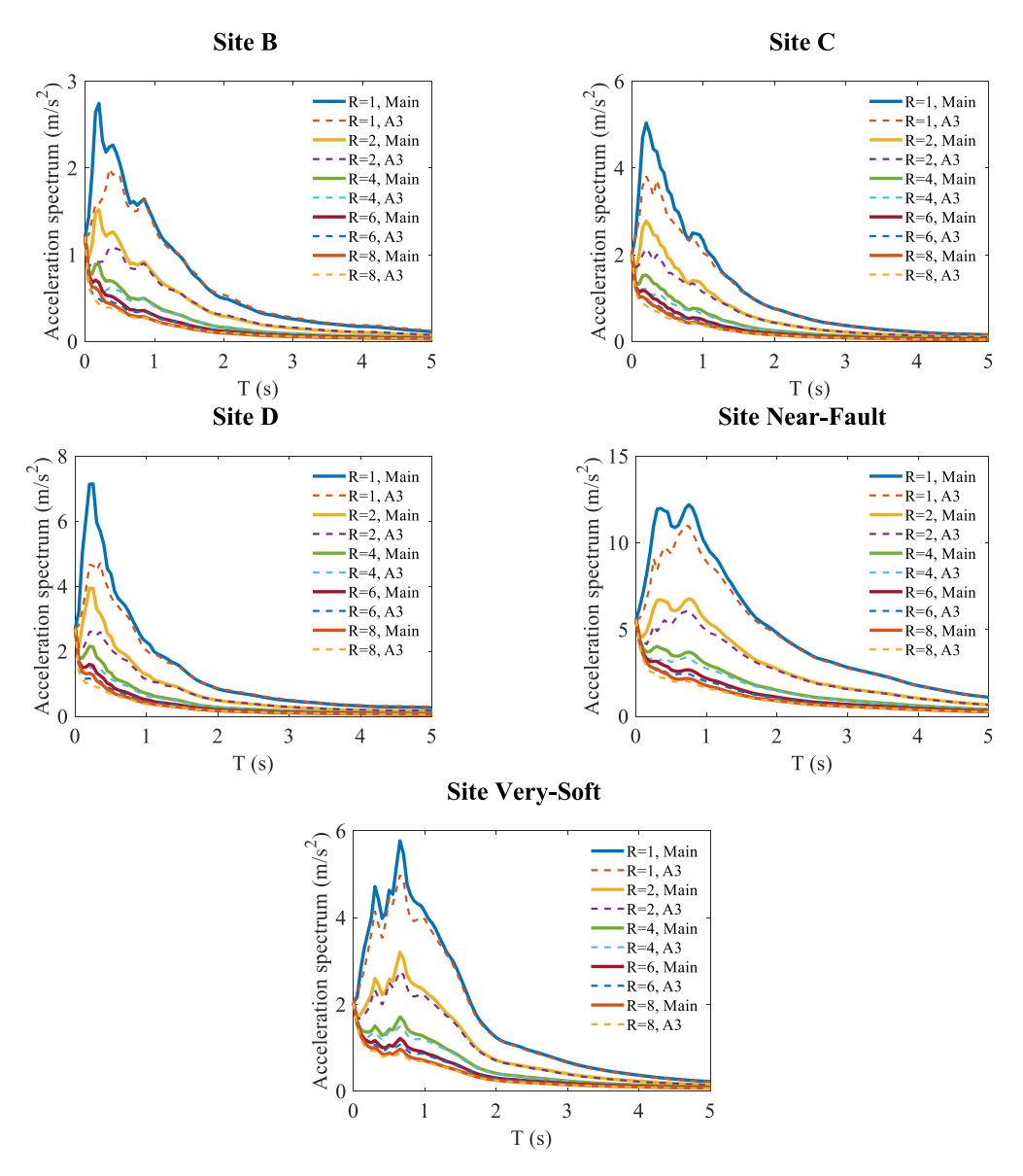


Fig. 15. Mean elastic acceleration response spectra of the main records and approximate ones obtained from the WTSC method.



 $\textbf{Fig. 16.} \ \ \text{Mean elastic and inelastic acceleration response spectra of the main records and A3 waves obtained from the WTSC method (R=1, 2, 4, 6, and 8). \\$

Table 3
Maximum error of different sites for the WTSC method.

Maximum error o	f mean acceleration spectrum	for soil type B (%)				
Wave	R = 8	R = 6	R = 4	R = 2	R = 1	
A1	8.09	7.41	6.37	8.38	6.51	
A2	16.19	19.62	22.92	25.27	24.97	
A3	25.31	28.10	34.17	39.87	42.14	
Maximum error o	f mean acceleration spectrum	for soil type C (%)				
Wave	R = 8	R = 6	R = 4	R = 2	R = 1	
A1	2.58	2.71	3.18	3.45	3.11	
A2	7.38	8.11	10.40	12.13	12.47	
A3	16.43	18.42	22.04	24.71	24.44	
Maximum error o	f mean acceleration spectrum	for soil type D (%)				
Wave	R = 8	R = 6	R = 4	R = 2	R = 1	
A1	4.09	4.21	4.37	4.48	4.87	
A2	15.03	17.06	19.09	21.31	21.30	
A3	25.19	27.78	30.73	34.05	35.96	
Maximum error o	f the mean acceleration spectr	um for the near-fault site (%)				
Wave	R = 8	R = 6	R = 4	R = 2	R = 1	
A1	0.97	0.98	1.33	2.15	2.93	
A2	6.46	8.11	8.41	11.26	13.18	
A3	16.35	18.15	21.66	26.51	29.61	
Maximum error o	f mean acceleration spectrum	for very soft soil (%)				
Wave	R = 8	R = 6	R = 4	R = 2	R = 1	
A1	1.22	1.29	1.35	1.87	2.03	
A2	4.71	5.19	5.70	8.33	9.03	
A3	10.65	11.74	12.58	13.91	15.04	

earthquake records listed in Table 5 and their approximate waves (A1 to A3) obtained from the three mentioned downsampling methods. As expected, application of the A3 wave greatly reduced the computational cost of the analyses. For example, using the A3 waves obtained from the WTSC method could reduce the computational cost by up to 90%. Table 6 shows the maximum error for estimating damper forces, base shear, and roof displacement of the structure for the A3 waves. The error in the estimation of roof displacement in the DWT method in one of the earthquake records has reached 11%, while it was less than 3% when the WTSC method was used. For other response parameters, the resulting errors of the TSC and the WTSC methods were less than the DWT method. The average error in the estimation of the above-mentioned response parameters for the A3 waves in the TSC and WTSC methods is less than 2%, while in the DWT method the average error is more than 5%. It can also be concluded that if the earthquake records with minimum error for SDOF systems are chosen, the error of all downsampling methods will be acceptable for this case study structure.

As an example, Fig. 20 illustrates the hysteresis curves of one of the dampers for two earthquake records and their approximate waves. Although there are differences in the hysteresis curves of approximate waves with the response of the original records, in general, the results compare very well. The best matching of the damper hysteresis curves is observed in the approximate waves obtained from the WTSC method, while the lowest matching is for the approximate waves obtained from the DWT method. A similar conclusion was obtained for other earthquake records and dampers.

5.2. Structure equipped with seismic isolators

In this section, a 15-story steel structure equipped with lead rubber bearings is considered. The plan and view of this structure are shown in Fig. 21. It should be mentioned that the plan of the structure is adopted from FEMA P-1051 [51]. The seismic isolators are designed based on the method presented by Constantinou et al. [53,54]. The specifications of the isolators are presented in Table 7. In this table, G is the elastic shear modulus of the rubbers, σ_{YL} is the lead core yield stress, k_d and $k_{d,total}$ are

the post-elastic stiffness for each isolator and the whole isolator system, respectively, Q_d and $Q_{d,total}$ are the yield strength of each isolator and the whole isolator system respectively, D_M , k_M , T_M , and β_M are the maximum displacement, effective stiffness, effective period and effective damping of the isolator system, respectively.

Table 8 presents the maximum errors for isolators forces, base shear, and roof displacement for the selected structure obtained based on time history analyses. It can be seen that, in general, the TSC and WTSC methods have better performance than the DWT method in this structure. Overall, the results indicate that the WTSC method provided the most reliable estimations with the average error close to 1% for all the response parameters. This is confirmed by comparison of the hysteresis curves of the isolators for the main records and the approximate waves as shown in Fig. 22.

6. Summary and conclusions

In this paper, the accuracy of three different downsampling methods for generating approximate earthquake records is examined for predicting the non-linear seismic response of complex structures. The downsampling methods considered include the discrete wavelet transform method (DWT) and the time step correction method (TSC), which were previously proposed, as well as the wavelet time step correction method (WTSC) that is presented in this paper for the first time. Linear and nonlinear response spectra of the original records and their approximate waves, filtered up to three levels, are compared for five sets of ground motions corresponding to different soil types. Subsequently, the practical applications of these methods are demonstrated for two case study structures, one equipped with viscous dampers and the other one equipped with seismic isolators. Based on the presented results, the following conclusions can be drawn:

 The proposed downsampling methods are not applicable for earthquake records with high frequency contents (above 5 Hz), especially if the DWT method is used. For such records, only one filtering step

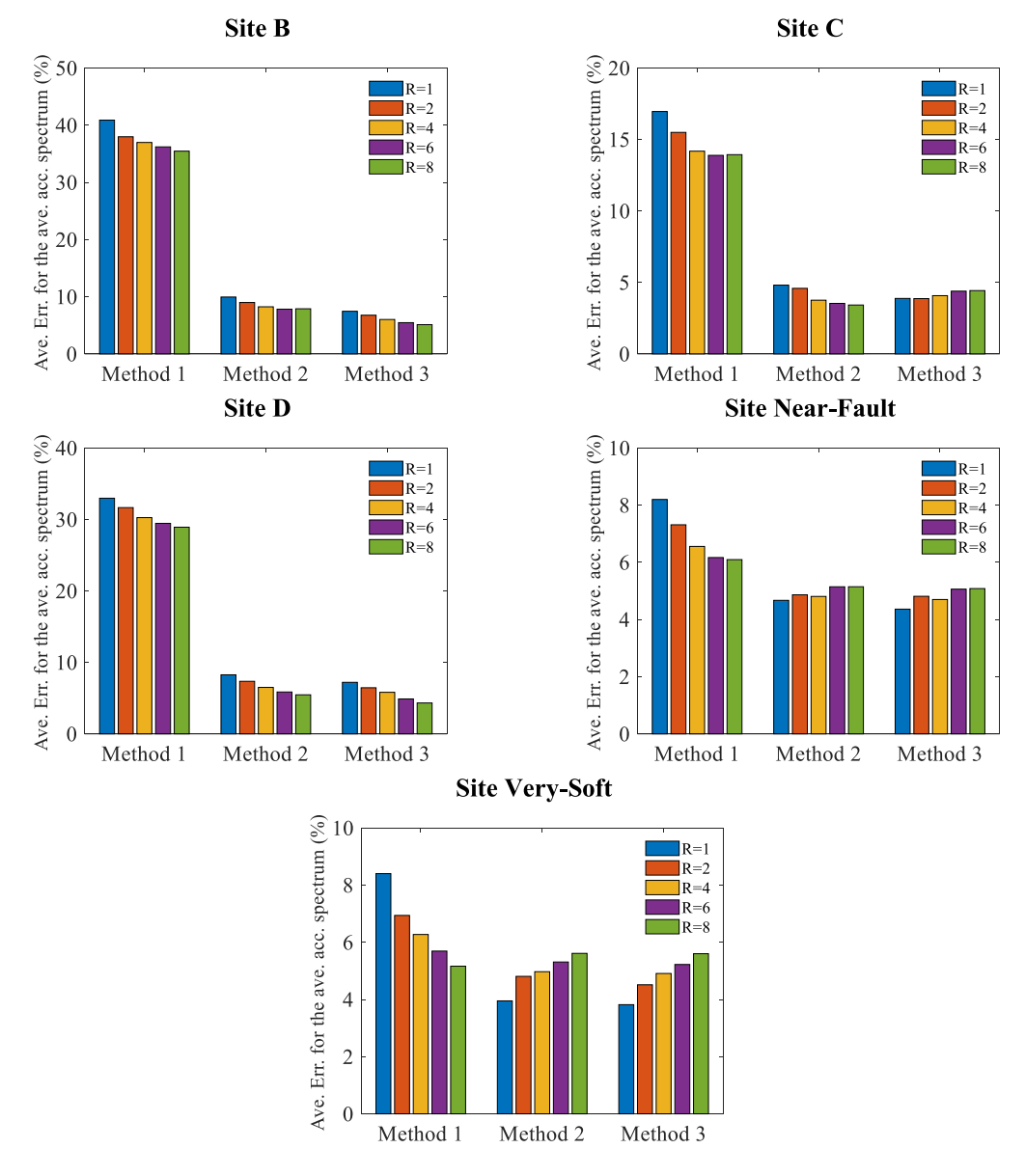


Fig. 17. Comparison of the average error of A3 waves for different methods.

 Table 4

 Computation time to obtain the acceleration response spectra for different behavior factors and different sites.

Wave	Computation time	(sec)			
	Site B	Site C	Site D	Near-Fault	Very soft soil
Main	1257	1306	1234	1006	1444
A1	677	686	663	553	815
A2	386	392	369	313	446
A3	262	242	241	205	278

Table 5 Specifications of selected earthquake records.

Name of the records	Earthquake	Station name	Site	Time Step	Magnitude (Ms)	NPTS	PGA (g)
E(1)	Loma Prieta	Anderson Dam, Downstream	С	0.005	7.1	7921	0.24
E(2)	Loma Prieta	Fremont, Mission San Jose	C	0.005	7.1	7990	0.12
E(3)	Loma Prieta	Gilroy, San Ysidro Microwave site	C	0.005	7.1	7991	0.17
E(4)	Morgan Hill	Gilroy, Gavilon College Phys Sci Bldg	C	0.005	6.1	7991	0.36
E(5)	Imperial Valley	Calexico, Fire Station	D	0.005	6.8	7561	0.28
E(6)	Loma Prieta	Hayward, John Muir School	D	0.005	7.1	7990	0.17
E(7)	Whittier Narrows	WNDWN180	D	0.005	6.1	7999	0.22

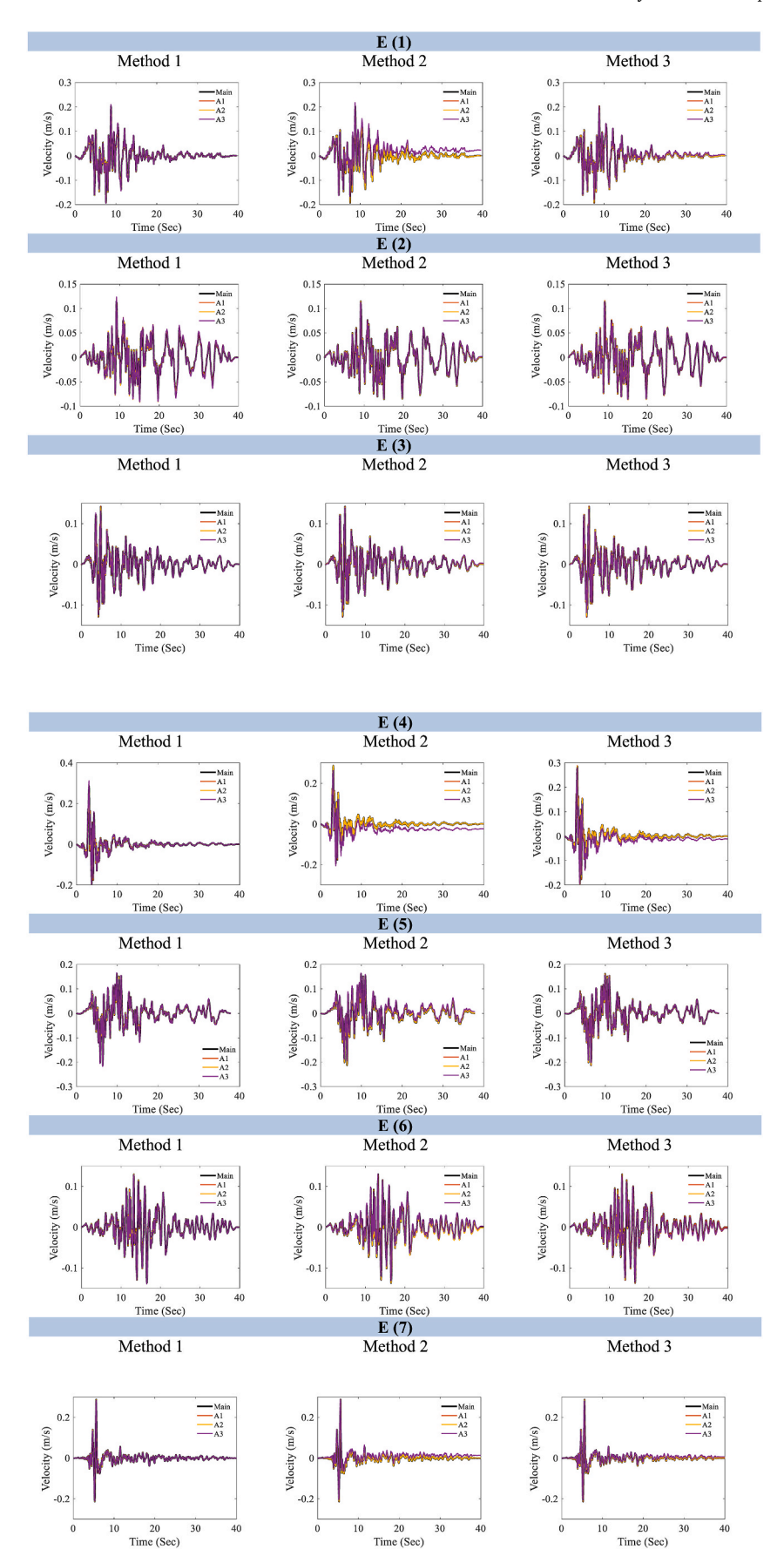


Fig. 18. Comparison of the velocity time history of seven selected earthquake records for different methods.



Fig. 19. Plan and view of the structure equipped with viscous dampers.

Table 6Results for viscous damper example errors.

Record	Method	Maximum damper force error (%)	Roof displacement error (%)	Base shear error (%)
E(1)	A3, DWT	1.37	6.31	3.21
	A3, TSC	0.53	1.18	1.57
	A3, WTSC	0.08	0.57	1.40
E(2)	A3, DWT	2.97	9.49	7.71
	A3, TSC	1.78	0.32	0.44
	A3, WTSC	1.55	1.21	0.90
E(3)	A3, DWT	0.41	1.05	1.34
	A3, TSC	1.46	4.36	0.98
	A3, WTSC	1.22	2.84	0.41
E(4)	A3, DWT	3.23	11.06	4.67
	A3, TSC	2.48	1.88	2.75
	A3, WTSC	2.15	0.68	1.01
E(5)	A3, DWT	1.42	5.37	2.67
	A3, TSC	3.50	0.21	1.09
	A3, WTSC	4.17	0.79	2.72
E(6)	A3, DWT	0.26	3.13	1.14
	A3, TSC	1.07	0.78	2.86
	A3, WTSC	1.35	0.16	2.15
E(7)	A3, DWT	0.29	1.58	0.55
	A3, TSC	0.99	1.87	1.98
	A3, WTSC	1.00	0.19	3.03
Error Average	A3, DWT	1.41	5.42	3.03
Ü	A3, TSC	1.68	0.95	1.66
	A3, WTSC	1.64	0.91	1.65

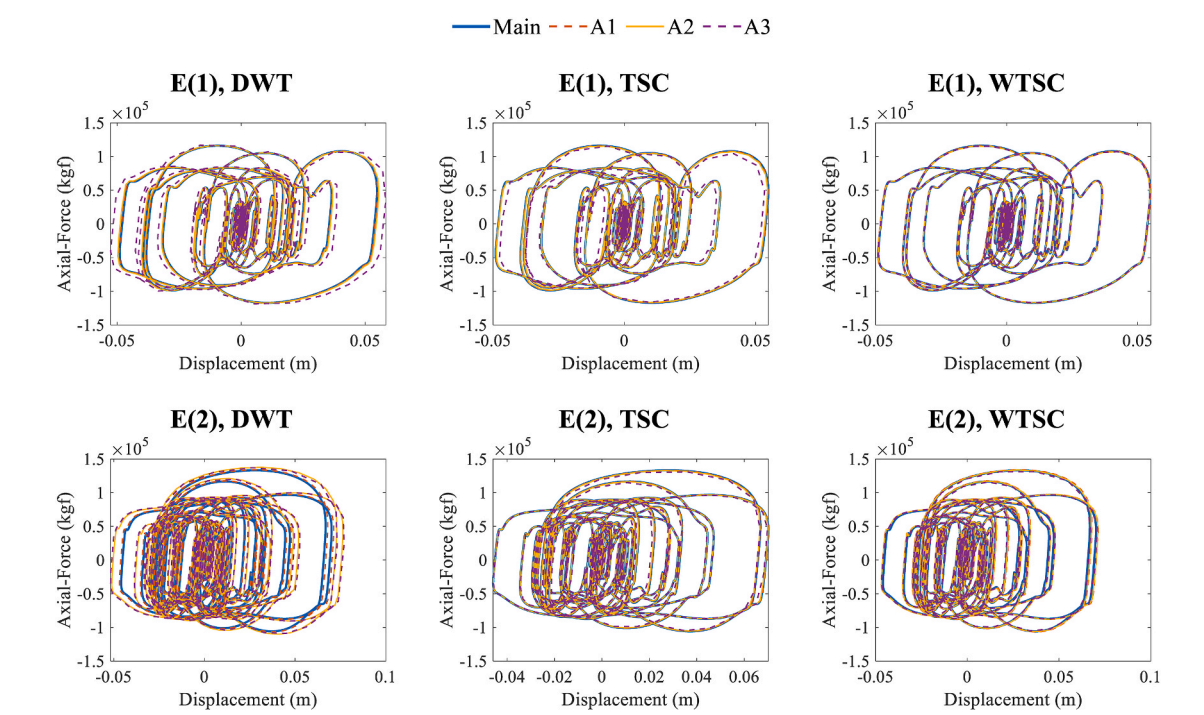


Fig. 20. Damper hysteresis curves.

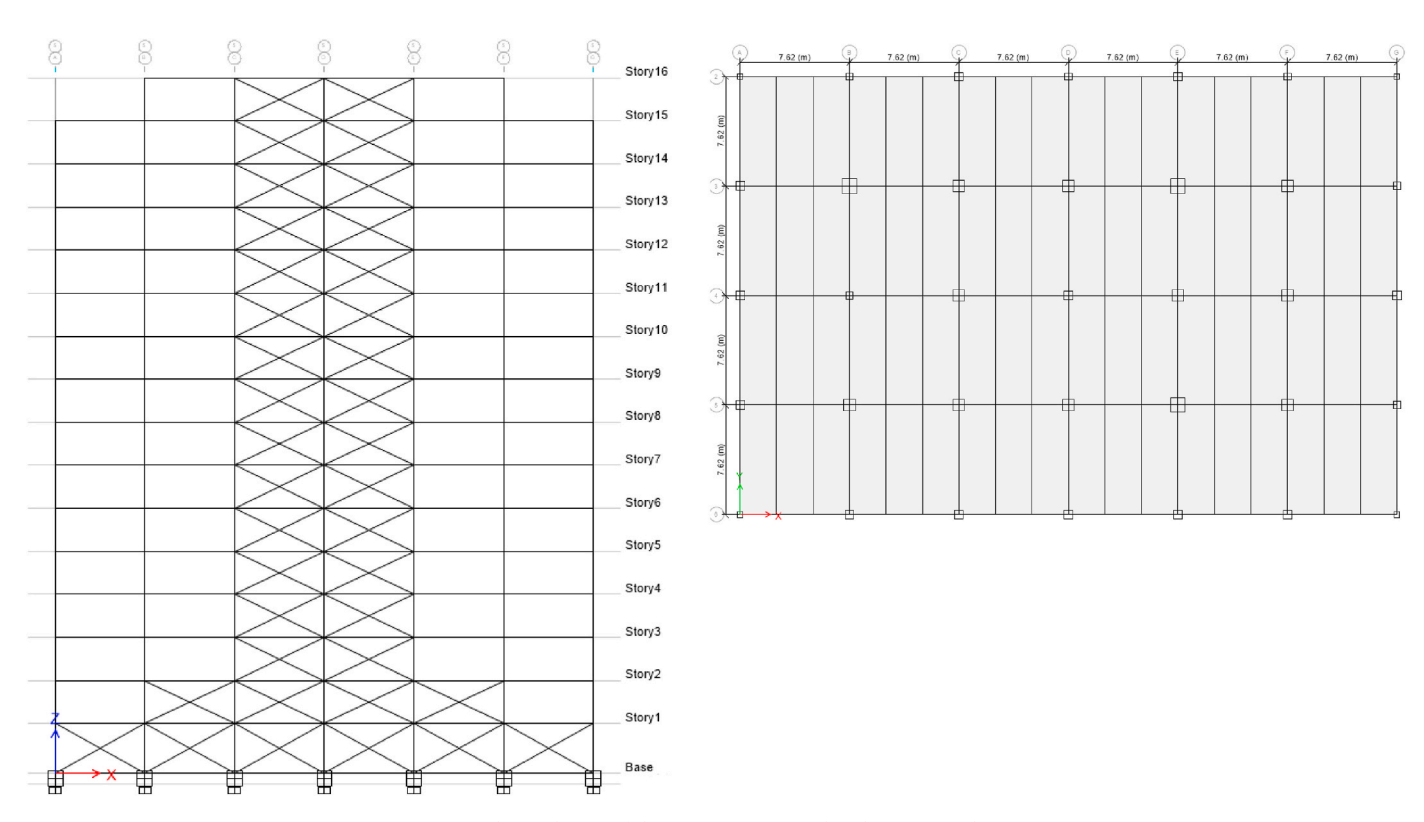


Fig. 21. Plan and view of the structure equipped with seismic isolators.

Table 7Lead rubber bearings specifications.

Isolator para	Isolator parameters										
G (ksi) 0.054	σ _{YL} (ksi) 1.16	k _d (kips/in) 9.66	$k_{d,total} \ (kips/in) \ 338.27$	Q _d (kips) 113.35	$Q_{d,total} \ (extit{kips}) \ 3967.40$	D _M (in) 20.00	$k_{\rm M}$ (kips/in) 536.20	T _M (sec) 2.90	$ \beta_{M} $ (%) 23.00		

Table 8Results for base isolator example errors.

Record	Method	Maximum isolator force error (%)	Roof displacement error (%)	Base shear error (%)
E(1)	A3, DWT	2.76	6.35	2.77
	A3, TSC	3.47	8.71	3.47
	A3, WTSC	0.86	2.25	0.87
E(2)	A3, DWT	2.01	4.73	2.07
	A3, TSC	0.06	0.23	0.08
	A3, WTSC	0.38	1.15	0.40
E(3)	A3, DWT	1.43	2.39	1.48
	A3, TSC	0.67	0.01	0.67
	A3, WTSC	0.11	0.27	0.12
E(4)	A3, DWT	5.94	10.10	5.95
	A3, TSC	0.05	2.01	0.14
	A3, WTSC	2.42	1.21	2.48
E(5)	A3, DWT	3.78	4.79	3.78
	A3, TSC	0.64	0.77	0.64
	A3, WTSC	0.24	0.41	0.24
E(6)	A3, DWT	2.15	2.09	2.16
	A3, TSC	0.31	0.38	0.33
	A3, WTSC	1.36	0.40	1.40
E(7)	A3, DWT	1.16	1.96	1.17
	A3, TSC	0.01	5.10	0.04
	A3, WTSC	1.86	1.72	1.85
Error Average	A3, DWT	2.74	4.62	2.76
· ·	A3, TSC	0.74	2.45	0.78
	A3, WTSC	1.02	1.05	1.04

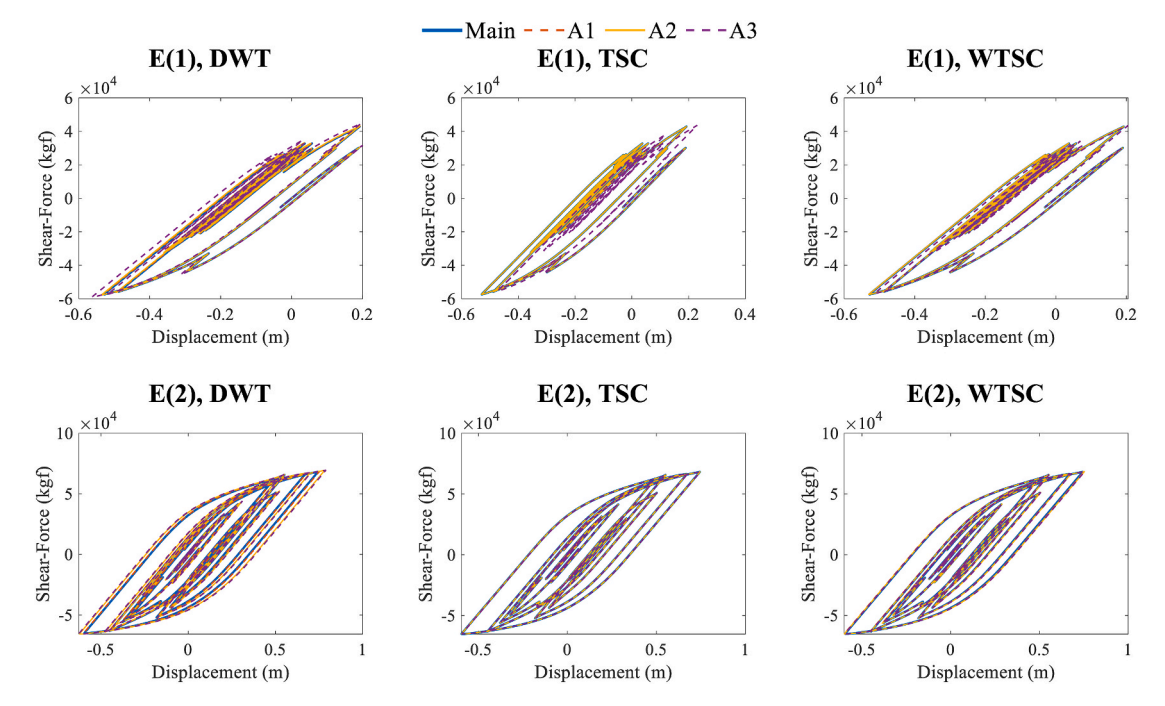


Fig. 22. Isolator hysteresis curves for two records.

for the DWT method and two filtering steps for the TSC and WTSC methods are recommended.

- The resulting error of all the three downsampling methods is affected
 by the soil type. The use of the TSC and WTSC methods is acceptable
 for all soil profiles when the A3 approximate waves are used. However, in the case of DWT method, using the A2 approximate waves
 leads to more accurate results.
- In general, regardless of the adopted downsampling method, the maximum errors were observed in the structures with a period less than 1 s. As the nonlinear behavior of the structures increases, the accuracy of all the downsampling methods generally increases. This indicates that changes in the dynamic characteristics of non-linear systems can be reasonably disregarded in practical applications.

• It is suggested to select earthquake records with the lowest error in their approximate waves based on the results of SDOF systems. It is shown that if these approximate waves are used in nonlinear time history analysis of complex structural systems, all the three downsampling methods lead to acceptable results while they can considerably reduce the computational costs of the analyses by 90%. However, it is shown that the proposed WTSC method clearly outperforms the DWT and TSC methods and can predict the non-linear seismic response parameters with an average error between 1 and 2%.

Author statement

Noorollah Majidi: Formal analysis, Investigation, Methodology,

Software, Writing-Original draft preparation.

Hossein Tajmir Riahi: Conceptualization, Methodology, Supervision, Validation, Visualization, Writing- Original draft preparation.

Sayed Mahdi Zandi: Conceptualization, Supervision, Visualization, Writing- Reviewing and Editing.

Iman Hajirasouliha: Validation, Visualization, Writing- Reviewing and Editing.

Declaration of competing interest

The authors declare that they have no known competing financial interests or personal relationships that could have appeared to influence the work reported in this paper.

Data availability

Data will be made available on request.

References

- [1] Clough RW, Penzien J. Dynamics of structures. MacGraw-Hill, Inc Editor; 1993.
- [2] McNamara J. Solution schemes for problems of nonlinear structural dynamics 1974.
- [3] Lülf FA, Tran D-M, Ohayon R. Reduced bases for nonlinear structural dynamic systems: a comparative study. J Sound Vib 2013;332(15):3897–921.
 [4] Meyer M, Matthies HG. Efficient model reduction in non-linear dynamics using the
- [4] Meyer M, Matthies HG. Efficient model reduction in non-linear dynamics using the Karhunen-Loeve expansion and dual-weighted-residual methods. Comput Mech 2003;31(1–2):179–91.
- [5] Toffolo A, Masi M, Lazzaretto A. Low computational cost CFD analysis of thermoacoustic oscillations. Appl Therm Eng 2010;30(6–7):544–52.
- [6] Hemez FM, Doebling SW. Review and assessment of model updating for non-linear, transient dynamics. Mech Syst Signal Process 2001;15(1):45–74.
- [7] Kaneko Y, Ito Y, Chow B, Wallace LM, Tape C, Grapenthin R, D'Anastasio E, Henrys S, Hino R. Ultra-long duration of seismic ground motion arising from a thick, low-velocity sedimentary wedge. J Geophys Res Solid Earth 2019;124(10): 10347–59
- [8] Lingfeng K, Maosheng G, Zhanxuan Z. The effect of duration of strong ground motion on the ductility demand of SDOF structure. In: IOP conference series: earth and environmental science. IOP Publishing; 2019.
- [9] Rupakhety R, Sigbjörnsson R. Rotation-invariant mean duration of strong ground motion. Bull Earthq Eng 2014;12(2):573–84.
- [10] Trifunac MD, Brady AG. A study on the duration of strong earthquake ground motion. Bull Seismol Soc Am 1975;65(3):581–626.
- [11] Soroushian A. A technique for time integration analysis with steps larger than the excitation steps. Commun Numer Methods Eng 2008;24(12):2087–111.
- [12] Nateghi F. On less computational costs for analysis of silos seismic behavior by time integration. In: Computational methods in structural dynamics and earhquake engineering; 2011.
- [13] Soroushian A, Saaed A, Arghavani M, Rajabi M, Sharifpour M. Less computational costs in the analysis of reservoirs seismic behaviors by time integration. In: Vibration problems ICOVP 2011: the 10th international conference on vibration problems. ICOVP 2011 Supplement; 2011. p. 205.
- [14] Hosseini M, Moghaddam SA, Emami SMM. A method for simplification of earthquake accelerograms for rapid time history analysis based on time-frequency representations. In: Conference: proceedings of the 11th international conference on vibration problems. ICoVP); 2013.
- [15] Yamamoto Y, Baker JW. Stochastic model for earthquake ground motion using wavelet packets. Bull Seismol Soc Am 2013;103(6):3044–56.
- [16] Salajegheh E, Heidari A. Dynamic analysis of structures against earthquake by combined wavelet transform and fast Fourier transform. Asian J Civil Eng 2002;3 (3&4):75–87.
- [17] Salajegheh E, Heidari A. Time history dynamic analysis of structures using filter banks and wavelet transforms. Comput Struct 2005;83(1):53–68.
- [18] Salajegheh E, Heidari A. Optimum design of structures against earthquake by wavelet neural network and filter banks. Earthq Eng Struct Dynam 2005;34(1): 67–82.
- [19] Heidari A, Raeisi J, Pahlavan Sadegh S. Dynamic analysis of shear building structure using wavelet transform. J Num Methods Civil Eng 2018;2(4):20–6.
- [20] Heidari A, Pahlavan sadegh S, Raeisi J. Investigating the effect of soil type on non-linear response spectrum using wavelet theory. Int J Civ Eng 2019;17(12): 1909–18.
- [21] Kaveh A, Aghakouchak A, Zakian P. Reduced record method for efficient time history dynamic analysis and optimal design. Earthquake Struct 2015;35:637–61.

- [22] Dadkhah M, Kamgar R, Heidarzadeh H. Reducing the cost of calculations for incremental dynamic analysis of building structures using the discrete wavelet transform. J Earthq Eng 2020:1–26.
- [23] Zealand SN. Structural design actions, Part 5: earthquake actions, vol. 5; 2004. NZS1170.
- [24] Belytschko T, Hughes TJ. Computational methods for transient analysis. Amsterdam: North-Holland(Computational Methods in Mechanics.; 1983. p. 1.
- [25] Lardies J, Gouttebroze S. Identification of modal parameters using the wavelet transform. Int J Mech Sci 2002;44(11):2263–83.
- [26] Iyama J, Kuwamura H. Application of wavelets to analysis and simulation of earthquake motions. Earthq Eng Struct Dynam 1999;28(3):255–72.
- [27] Kiyani K, Raeisi J, Heidari A. Time-frequency localization of earthquake record by continuous wavelet transforms. Comput Engineering and Phys Model 2019;2(2): 50–60.
- [28] Huang D, Wang G. Stochastic simulation of regionalized ground motions using wavelet packets and cokriging analysis. Earthq Eng Struct Dynam 2015;44(5): 775–94.
- [29] Baker JW. Quantitative classification of near-fault ground motions using wavelet analysis. Bull Seismol Soc Am 2007;97(5):1486–501.
- [30] He W-Y, Wang Y, Ren W-X. Dynamic force identification based on composite trigonometric wavelet shape function. Mechanical Systems and Signal Processing; 2019, 106493.
- [31] Jiang X, Mahadevan S. Wavelet spectrum analysis approach to model validation of dynamic systems. Mech Syst Signal Process 2011;25(2):575–90.
- [32] Schneider K, Vasilyev OV. Wavelet methods in computational fluid dynamics. Annu Rev Fluid Mech 2010;42:473–503.
- [33] Mahdavi SH, Abdul Razak H. Indirect time integration scheme for dynamic analysis of space structures using wavelet functions. J Eng Mech 2015;141(7):04015006.
- [34] Heidari A, Majidi N. Earthquake mapping acceleration analysis using wavelet method, earthquake engineering and engineering vibration. 2019.
- [35] Kamgar R, Dadkhah M, Naderpour H. Seismic response evaluation of structures using discrete wavelet transform through linear analysis. Structures 2021;29: 863–82
- [36] Kamgar R, Majidi N, Heidari A. Wavelet-based decomposition of ground acceleration for efficient calculation of seismic response in elastoplastic structures. Periodica Polytechnica Civil Engineering; 2020.
- [37] Heidari A, Raeisi J. Investigating the effect of soil type on non-linear response spectrum using wavelet theory. Int J Civ Eng 2019;17(12):1909–18.
- [38] Heidari A, Salajegheh E. Time history analysis of structures for earthquake loading by wavelet networks. Asian J Civil Eng 2006;7.
- [39] Mallat S. A wavelet tour of signal processing. Elsevier; 1999.
- [40] Misiti M, Misiti Y, Oppenheim G, Poggi J-M. Wavelet toolbox user's guide. The Math Works Inc; 1996.
- [41] Soroushian A, Farahani EM. Efficient static analysis of assemblies of beam-columns subjected to continuous loadings available as digitized records. Frontier Built Environ. 2019;4:83.
- [42] Soroushian A. A general rule for the influence of physical damping on the numerical stability of time integration analysis. J Appl Comput Mech 2018;4: 467–81. Special Issue: Applied and Computational Issues in Structural Engineering.
- [43] Soroushian A, Hosseini M, Khalkhali smh. On the frequency content of errors originated in a time integration computational cost reduction technique. In: Conference: ECCOMAS congress 2016. VII European Congress on Computational Met hods in Applied Sciences and Engineerin; 2016.
- [44] Soroushian A, Farshadmanesh P, Azad S. On the essentiality of techniques to enlarge integration steps in transient analysis against digitized excitations. J Seismol Earthquake Eng 2016;17(1):43–60.
- [45] Soroushian A. A general practical procedure for a recently proposed seismic analysis computational cost reduction technique. In: Proceedings of 7th international conference on seismology and earthquake engineering. Tehran, Iran: SEE7): 2015.
- [46] Zarabimanesh Y, Khalkhali M, Soleymani K, Akbarnejad F, Mirghaderi R, Soroushian A. On reduction of computational cost in transient analysis of structures against near field earthquakes. In: 6th ECCOMAS thematic conference on computational methods in structural dynamics and earthquake engineering (COMPDYN 2017); 2017. Rhodes, Greece.
- [47] Fema A. Improvement of nonlinear static seismic analysis procedures. 440 FEMA-440 2005;7(9):11. Redwood City.
- [48] Engineers ASoC. Minimum design loads and associated criteria for buildings and other structures. American Society of Civil Engineers; 2017.
- [49] Jennings PC, Housner GW, Tsai NC. Simulated earthquake motions. 1968.
- [50] Thomas S, Pillai G, Pal K, Jagtap P. Prediction of ground motion parameters using randomized ANFIS (RANFIS). Appl Soft Comput 2016;40:624–34.
- [51] Agency FEM. 2015 NEHRP recommended seismic provisions: design examples. Washington, DC: FEMA P-1051; 2015.
- [52] Christopoulos C, Filiatrault A. Principles of passive supplemental damping and seismic. Pavia, Italy: IUSS Press; 2006.
- [53] Constantinou MC, Kalpakidis IV, Filiatrault A, Lay RE. LRFD-based analysis and design procedures for bridge bearings and seismic isolators. MCEER; 2011.
- [54] Constantinou MC, Whittaker A, Kalpakidis Y, Fenz D, Warn GP. Performance of seismic isolation hardware under service and seismic loading. Technical Rep. No. MCEER- 2007;7:12.